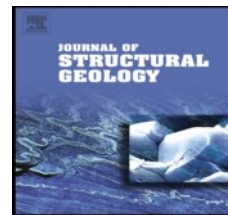


## Accepted Manuscript

Title: The kinematic history of the Khlong Marui and Ranong Faults, Southern Thailand

Authors: Ian Watkinson, Chris Elders, Robert Hall

PII: S0191-8141(08)00148-X  
DOI: [10.1016/j.jsg.2008.09.001](https://doi.org/10.1016/j.jsg.2008.09.001)  
Reference: SG 2186



To appear in: *Journal of Structural Geology*

Received Date: 19 February 2008

Revised Date: 1 September 2008

Accepted Date: 9 September 2008

Please cite this article as: Watkinson, I., Elders, C., Hall, R. The kinematic history of the Khlong Marui and Ranong Faults, Southern Thailand, *Journal of Structural Geology* (2008), doi: 10.1016/j.jsg.2008.09.001

This is a PDF file of an unedited manuscript that has been accepted for publication. As a service to our customers we are providing this early version of the manuscript. The manuscript will undergo copyediting, typesetting, and review of the resulting proof before it is published in its final form. Please note that during the production process errors may be discovered which could affect the content, and all legal disclaimers that apply to the journal pertain.

1 The kinematic history of the Khlong Marui and Ranong Faults, Southern  
2 Thailand

3

4 Ian Watkinson\*, Chris Elders, Robert Hall

5 *SE Asia Research Group, Department of Geology, Royal Holloway, University*  
6 *of London, Egham, Surrey, TW20 0EX, United Kingdom*

7

8 **Abstract**

9 The Khlong Marui Fault (KMF) and Ranong Fault (RF) are major NNE  
10 trending strike-slip faults which dissect peninsular Thailand. They have been  
11 assumed to be conjugate to the NW-trending Three Pagodas Fault (TPF) and  
12 Mae Ping Fault (MPF) in Northern Thailand, which experienced a diachronous  
13 reversal in shear sense during India – Eurasia collision. It follows that the KMF  
14 and RF are expected to show the opposite shear sense and an inversion at a  
15 similar time to the TPF and MPF. New field data from the KMF and RF reveal  
16 two phases of ductile dextral shear separated by Campanian magmatism.  
17 Paleocene to Eocene post-kinematic granites date the end of this phase, while a  
18 brittle sinistral phase deforms the granites, and has exhumed the metamorphic  
19 rocks. The timing of these movements precludes formation of the faults in  
20 response to Himalayan extrusion tectonics. Instead, they formed near the  
21 southern margin of a late Cretaceous – Paleocene orogen, and may have been

\* Corresponding author. *SE Asia Research Group, Department of Geology, Royal Holloway, University of London, Egham, Surrey, TW20 0EX, United Kingdom. Tel: +441784 443611; fax: +441784 434716. E-mail address: i.watkinson@gl.rhul.ac.uk (Ian Watkinson).*

22 influenced by variations in the rate of subduction ahead of India and Australia.  
23 North-south compression prior to reactivation of the subduction zone around  
24 southern Sundaland in the Eocene caused widespread deformation in the over-  
25 riding plate, including sinistral transpression on the KMF and RF.

26

## 27 **Keywords**

28 Strike-slip faults; Fault kinematics; Lateral extrusion; Ductile shear zone;  
29 Thailand; Sundaland

## 30 **1.0 Introduction**

31 Widespread intraplate deformation within mainland Southeast Asia is  
32 conspicuously expressed by northwest trending strike-slip faults which  
33 originate near the eastern Himalayan syntaxis. These include the Ailao Shan –  
34 Red River Fault (ASRR), the Mae Ping Fault (MPF), and the Three Pagodas  
35 Fault (TPF) (Fig. 1), which are interpreted to have played a key role in the  
36 eastwards movement of fault-bounded blocks during indentation of the Indian  
37 continent into the Eurasian plate (e.g. Gilley et al., 2003; Lacassin et al., 1997;  
38 Leloup et al., 1995; Tapponnier et al., 1982, 1986). They record a history of  
39 sinistral motion under medium to high metamorphic conditions followed by a  
40 diachronous reversal in shear sense and a change to brittle deformation during  
41 the Oligocene on the TPF and MPF, and the Miocene on the ASRR (Gilley et  
42 al., 2003; Lacassin et al., 1997; Leloup et al., 1995, 2001; Wang et al., 1998).  
43 Northward-younging slip sense reversal is believed to result from northward

44 migration of the Himalayan deformation front and lateral extrusion of  
45 successive fault-bounded blocks (Lacassin et al., 1997).

46 The northeast-trending Khlong Marui Fault (KMF) and Ranong Fault  
47 (RF) (Fig. 2) cut across the Thai Peninsula south of the NW trending faults, and  
48 are orientated about  $100^\circ$  anti-clockwise of the TPF (Fig. 1). Although they  
49 have not been traced offshore, the two fault zones appear to intersect in the  
50 northern Gulf of Thailand. As a result, the KMF and RF have been interpreted  
51 to be conjugate to the TPF and MPF (Lacassin et al., 1997; Tapponnier et al.,  
52 1986), an assumption which has become entrenched in subsequent references to  
53 the Tertiary deformation of the area. Their kinematics are therefore modeled as  
54 ductile dextral motion during the early stages of India – Eurasia collision,  
55 changing to brittle sinistral at the same time as the change from sinistral to  
56 dextral on the TPF and MPF (e.g. Hall, 1996, 2002; Lee and Lawver, 1995;  
57 Replumaz and Tapponnier, 2003; Tapponnier et al., 1986).

58 Development of the South China Sea, and Tertiary basins of offshore  
59 Vietnam, Cambodia and in Northern Thailand, have also been attributed to  
60 movement on the NW-trending strike-slip faults (Briaies et al., 1993, Polachan et  
61 al., 1991; Tapponnier et al., 1986), and offshore extensions of the KMF and RF  
62 have been linked to extension in the Andaman Sea and the Gulf of Thailand  
63 (e.g. Packham, 1993; Pigott and Sattayarak, 1993; Polachan, 1988). However,  
64 the timing and extent of deformation on the NW trending structures is still  
65 under debate (e.g. England and Houseman, 1986; Hall and Morley, 2004;  
66 Rangin et al., 1995; Searle, 2006), and recent workers have favoured processes

67 such as subduction rollback (Morley, 2001), lower crustal flow (Morley and  
68 Westaway, 2006), and changing intraplate stresses as a result of edge forces  
69 (Hall and Morley, 2004), as principal controls on extension in the basins,  
70 reducing the importance of large strike-slip faults in the evolution of Southeast  
71 Asia.

72 The KMF and RF have undoubtedly played a part in this evolution.  
73 Early work on the KMF identified a phase of brittle sinistral strike-slip  
74 deformation, based on the apparent offset of granites across the fault (Garson  
75 and Mitchell, 1970). Detailed field-based studies of fault kinematics have been  
76 notably lacking, until Intawong (2006) recognised an additional, older, ductile  
77 phase.

78 This paper presents new field evidence supporting these events on the  
79 KMF, and a similar change from ductile dextral to brittle sinistral shear on the  
80 larger, less well studied RF. Integrating this new field data with existing ages  
81 shows that the ductile phase pre-dates Himalayan deformation, and therefore  
82 the connection to the northern faults is more complicated than previously  
83 assumed.

## 84 **2.0 Geological setting**

### 85 *2.1 The Thai Peninsula*

86 The structural geology of the N-S trending Thai Peninsula is dominated  
87 by the KMF and RF: broadly linear NNE-trending strike-slip fault zones  
88 centered around elongate slivers of metamorphic fault rocks (Fig. 2). These are

89 bounded and overprinted by brittle strands, which are part of a population of  
90 parallel and branching sinistral faults which are localised into the two similar  
91 but discrete fault zones. The smaller KMF passes from Ko Phuket in the south  
92 towards Surat Thani in the north, while strands of the RF can be traced from  
93 Takua Pa in the south to Pran Buri in the north, crossing the peninsula entirely.  
94 A relatively undeformed block with a strike-normal width of no more than 50  
95 km lies between the two faults.

96           Rocks in and around the fault zones are dominantly late Palaeozoic  
97 marine sediments deposited at mid-southern latitudes (Metcalf, 2002, 2006).  
98 Most prominent are siliciclastic deposits of the Permo-Carboniferous Kaeng  
99 Krachan or Phuket Group, the oldest exposed rocks in the fault zone, which  
100 occupy a broad area of the central Thai Peninsula (Department of Mineral  
101 Resources, 1982). They comprise grey mudstone, siliceous shale, sandstone,  
102 and conglomeratic sequences between two and three km thick. Distinctive  
103 pebbly mudstones, interpreted as diamictites (Bunopas et al., 1991), are  
104 ubiquitous to the north of the KMF, and can be recognised even where they  
105 have been strongly deformed in the ductile shear zones. However, they rarely  
106 occur in the Permo-Carboniferous succession south of the fault zone.

107           Permian Ratburi Group carbonates overlie the Kaeng Krachan Group  
108 with either a locally conformable or unconformable contact (Garson et al.,  
109 1975; Bunopas et al., 1991). They are exposed as tropical tower karsts (Baird  
110 and Bosence, 1993), the long axes of which typically parallel the NNE-SSW  
111 structural trend on the peninsula. Sandstones and shales of the Jurassic to

112 Cretaceous Thung Yai Group crop out on the eastern side of the RF, and all  
113 lithologies are progressively overlain by Quaternary deposits as topographic  
114 relief decreases towards the Gulf of Thailand (Department of Mineral  
115 Resources, 1982, 2006).

## 116 *2.2 Regional context*

117 The Thai Peninsula lies near the western edge of Sundaland, the  
118 southeastern promontory of the Eurasia plate which is bounded by active  
119 oceanic spreading centres, strike-slip faults, and pre-Cenozoic sutures (Hall and  
120 Morley, 2004). Sundaland's coherence was attained in the Late Cretaceous,  
121 following a prolonged period of collision between allochthonous fragments  
122 derived from the Palaeozoic supercontinent Gondwana (e.g. Lepvrier et al.,  
123 2004; Metcalfe, 1991, 1996, 2006). Four major terranes make up mainland  
124 Southeast Asia. These are South China, Indochina, East Malaya, and Sibumasu  
125 (Metcalfe, 1991), within which the KMF and RF have formed. Additionally,  
126 several smaller terranes, including the West Burma and West Sumatra blocks, a  
127 continental fragment below East Java, and the fragments that form the Mawgyi  
128 and Woyla nappes are interpreted to have accreted to the western and southern  
129 edges of Sundaland during the Mesozoic (e.g. Barber, 2000; Metcalfe, 1996;  
130 Mitchell, 1993; Smyth et al., 2007).

131 Magmatism attributed to this prolonged phase of subduction, collision  
132 and crustal thickening occurred across eastern Myanmar, western Thailand,  
133 peninsular Malaysia and Sumatra. Granitoids rich in ore deposits occur as  
134 stocks and N-S trending elongate batholiths, arranged into three

135 geochronologically and petrologically distinct N-S trending bands: the Western,  
136 Main Range, and Eastern Granite Provinces (e.g. Charusiri, 1989; Cobbing et  
137 al., 1986; Hutchison, 1989; Putthapiban and Schwartz, 1994; Ridd, 1978). The  
138 granites range from small I-type Permo-Triassic intrusions in the east to larger  
139 S-type Palaeogene bodies in the west (Charusiri, 1989; Cobbing et al., 1986;  
140 Putthapiban and Schwartz, 1994). Granites of the Western Province lie within  
141 and around the KMF and RF, while Main Range granites crop out immediately  
142 SE of the KMF (Fig. 1 and Fig. 2).

### 143 **3.0 Deformation on the Khlong Marui and Ranong Faults**

144 Satellite imagery clearly reveals the position, orientation and scale of  
145 deformation across the fault zones, and reports of granites across the peninsula  
146 have alluded to fabrics attributed to strike-slip shear (e.g. Charusiri, 1989,  
147 Hutchison, 1989; Nakapadungrat et al., 1991; Putthapiban, 1992). The faults  
148 have consequently been included in models for the Tertiary tectonic evolution  
149 of Southeast Asia, including those of Tapponnier (1986), Lee and Lawver  
150 (1995), Hall (1996, 2002), and Replumaz and Tapponnier (2003), typically  
151 acting as a boundary between fragments representing the northern and southern  
152 parts of the Thai-Malay Peninsula. Displacement estimates have ranged from  
153 100 km of dextral offset on the KMF (Kornsawan and Morley, 2002) to at least  
154 200 km of sinistral offset (Garson and Mitchell, 1970); and from 200 km  
155 (Tapponnier et al., 1986) of dextral offset on the RF, to 20 km of sinistral offset  
156 (Garson and Mitchell, 1970). Ridd's (1978) estimate of combined sinistral  
157 displacement on the KMF and Kapoe Fault (part of the RF) was 250 km. The



158 timing of the dextral displacements is typically modeled according to the faults'  
159 hypothesised role as conjugate structures to the MPF and TPF, which were  
160 sinistral in the Oligocene (Lacassin et al., 1997). Recent field studies have  
161 shown that the KMF has experienced a change from ductile dextral to brittle  
162 sinistral strike-slip motion (Intawong, 2006), as has long been assumed. This  
163 paper demonstrates a similar change on the RF, and constraints on the timing of  
164 deformation phases across the whole of the KMF and RF.

165 The fault zones were mapped using a combination of detailed fieldwork  
166 in Thailand, 30 metre Landsat TM multi-spectral imagery and 90 metre Shuttle  
167 Radar Topography Mission (SRTM) Version 2 data for Thailand and Myanmar,  
168 1/250,000 scale aeromagnetic anomaly maps and Th, U, and total count  
169 radiation maps for Thailand. Sedimentary and intrusive rocks outside the fault  
170 zone shown on the fault maps are modified from 1/50,000 and 1/250,000 scale  
171 maps published by the Thai Department of Mineral Resources (1980, 1982,  
172 1992, 2006). Four phases of strike-slip deformation were identified ( $D_1$ ,  $D_2$ ,  $D_3$ ,  
173 and  $D_4$ ), which have similar orientation and expression in both fault zones.

174

### 175 3.1 $D_1$

176 Deformation phase 1 involved dominantly non-coaxial dextral strike-  
177 slip strain at low metamorphic grades, followed by folding of variable intensity.  
178 It is recorded by pelites and metaconglomerates of the Kaeng Krachan Group  
179 with a continuous cleavage or domain spaced cleavage  $S_1$  which strikes  
180 between  $000^\circ$  and  $035^\circ$  and dips variably to the east and west. Original

181 sedimentary bedding  $S_0$  is rarely discernable. A prominent lineation on  $S_1$   
182 typically plunges less than  $20^\circ$  and is defined by mica elongation and stretched  
183 clasts.

184 Fine grained micas define  $S_1$ , which flows smoothly around  
185 porphyroclasts of quartz, lithic fragments of sandstone and more rarely  
186 mudstone (Fig. 3a). Euhedral apatite within some quartz clasts indicates that  
187 they are derived directly from an igneous parent rock. Smaller quartz clasts are  
188 monocrystalline, with undulose extinction in random orientations, probably a  
189 record of pre-sedimentary deformation. Dissolution away from angular  
190 porphyroclast corners is expressed by rounding and seams of opaque insoluble  
191 material which form strain caps and enhance  $S_1$ . The fabric varies from  
192 cataclastic to mylonitic, and strain is rather variable. While matrix quartz  
193 typically does not show evidence of dynamic recrystallisation, zones of bulging  
194 and subgrain rotation recrystallisation are locally developed. Diffuse pressure  
195 shadows, formed by very small grains of recrystallised quartz and mica  
196 concentrations, are common around larger porphyroclasts and relict pebbles in  
197 areas of higher strain.

198 Asymmetric elongation of porphyroclasts, stair-stepping pressure  
199 shadows and mica fish indicate consistently dextral shear coeval with  $S_1$   
200 development. Rare C-S fabrics defined by superposition of dark dissolution  
201 seams on older S planes formed by mica alignment record the same shear sense.

202 Folding of  $S_1$  is highly variable, but typically involves asymmetric  
203 harmonic parallel and chevron folds and kink bands (Fig. 3b). These have axial

204 surfaces which dip to the SE, SW and N, and hinge lines which plunge  
205 moderately to the NW, NE and W. Folds develop on all scales including  
206 microscopic, but no secondary cleavage is associated with them. The style and  
207 orientation of folding shows that it occurred during a late stage of  $D_1$ , at lower  
208 metamorphic conditions than strike-slip deformation.

209 Structural relationships indicating that  $D_1$  is the first deformation event  
210 on the KMF and RF are unambiguous only at Ranong (Fig. 4). A well defined  
211 band of sheared and folded rocks are obliquely cut by the Ranong granite,  
212 which is itself cut by a younger, medium grade shear zone, attributed to  $D_2$ . At  
213 a number of other locations on the RF, similar fault rocks are intruded by dykes  
214 of the same latest Cretaceous age as the Ranong granite. Other areas interpreted  
215 to record  $D_1$  deformation, including those within the KMF, have been mapped  
216 based on the distinctive deformation style which is similar to that of the sheared  
217 and folded rocks at Ranong. While it is likely that  $D_2$  overprinted much of the  
218  $D_1$  shear zone, its intensity and duration were such that older fabrics in areas of  
219  $D_2$  deformation cannot be confidently attributed to  $D_1$ .

### 220 3.2 $D_2$

221 The most intense phase of deformation,  $D_2$ , was a period of non-coaxial  
222 dextral strike-slip strain at medium to high metamorphic grades. Rocks  
223 deformed by  $D_2$  are exposed within at least five elongate slivers of  
224 metamorphic rocks on the RF, while on the KMF, a single sliver is exposed  
225 (Fig. 2).  $D_2$  formed a widespread foliation  $S_2$  which strikes  $005^\circ$  to  $030^\circ$  and

226 dips both east and west at angles greater than 50°. Mineral stretching lineations  
227 developed on these planes plunge at a shallow angle to the NNE and SSW.

228

229 Five broad metamorphic lithologies were created by, or modified during  
230 deformation associated with D<sub>2</sub>. These are, in order of prevalence: poorly  
231 segregated, high melt migmatites; foliated granites and orthogneisses; well  
232 segregated, low melt migmatites; quartz-biotite mylonites; and a range of  
233 sheared meta-sediments.

### 234 *3.2.1 High melt volume migmatite*

235 High melt volume stromatic and nebulitic migmatites (Fig. 3c) are  
236 limited to the RF, and crop out discontinuously in two strands between Kra  
237 Buri and Bang Saphan (Fig. 5 and Fig. 6). They differ from the low melt  
238 migmatites not just in anatexis magnitude, but in mesosome texture.  
239 Mesosomes are medium grey in colour, coarser grained, contain more biotite  
240 and have a less schistose, more gneissic foliation. They contain finely  
241 disseminated leucocratic material, including isolated, large, well rounded K-  
242 feldspar phenocrysts with recrystallised feldspar and quartz sigma-type strain  
243 shadows. This indicates temperatures during shear above the brittle –  
244 crystalplastic transition for feldspar in wet rocks (~500°C) (Gapais, 1989;  
245 Passchier and Trouw, 2005). Leucosomes are typically wispy, poorly defined,  
246 and rarely bounded by melanosomes. K-feldspar and plagioclase again show  
247 evidence of crystalplastic flow, and there is extensive grain boundary migration  
248 in quartz crystals. Hornblende and garnet are commonly present, and deform by

249 brittle mechanisms, indicating temperatures during shearing below 700 °C.

250 Synthetic dextral shear bands between leucosome boudins are common.

### 251 *3.2.2 Foliated granites and orthogneisses*

252         The high melt volume migmatites always have a close spatial  
253 association with foliated granites. Deformation of the granites occurred under a  
254 range of metamorphic conditions, commonly within the greenschist facies.  
255 Locally pervasive S-C' fabrics illustrate progressive retrograde metamorphism  
256 during shearing in some of the foliated granites (Fig. 3d). Original S-planes are  
257 defined by foliation-parallel bands of coarse biotite which curve around  
258 deformed feldspar porphyroclasts. Feldspars deform in a brittle manner,  
259 expressed by micro- and macroscopic sinistral domino-style antithetic faults in  
260 subhedral K-feldspar phenocrysts, by microscopic tectonic abrasion of all  
261 feldspars, and by bent plagioclase twin lamellae. Recrystallised quartz shows  
262 undulose extinction, and is typically arranged into elongate polycrystalline  
263 aggregates, ribbons and tails emanating from rounded feldspar porphyroclasts.  
264 These structures display a clear dextral stair-stepping geometry at all scales of  
265 observation. Regular, closely spaced dextral C' planes reveal continued  
266 shearing under cooler conditions. They are dominated by small quartz grains  
267 formed by bulging recrystallisation, chlorite, clastic fragments of feldspar,  
268 euhedral zircons, and fine biotite fragments. Quartz was ductile in both of these  
269 phases, indicating temperatures not below ~ 300°C (Stipp et al., 2002) during  
270 all of the deformation associated with D<sub>2</sub>, a conclusion common to all of the  
271 rocks deformed during D<sub>2</sub>.

272 Biotite is not a major component of the interfolial domains, taken to  
273 represent protolith composition, so the large biotite crystals partly defining S-  
274 planes are interpreted to be syn-kinematic in origin, rather than reoriented  
275 magmatic crystals. The finely crushed mica in C'-planes probably originated in  
276 the S-planes, suggesting that no new biotite growth occurred during this  
277 younger period of deformation.

278 Crystalplastic deformation, deformation twins and subgrain  
279 development in feldspar porphyroclasts occurs in regions of higher grade  
280 metamorphism, together with extensive myrmekite, quartz grain boundary  
281 migration, and biotite rich pressure shadows. In some granites, S-C' fabrics do  
282 not record significant retrograde metamorphism, most notably near Khao  
283 Nakkharat, northwest of Bang Saphan. The younger C' planes here are defined  
284 by fine grained quartz ribbons, and mantled feldspar porphyroclasts, with  
285 dextral asymmetry. These show extensive crystalplastic deformation parallel to  
286 the shear planes. Titanite is concentrated in these planes, and is the only mineral  
287 that fractures in a brittle manner. Higher grade foliated granites such as these  
288 are essentially mylonitic orthogneisses, with S<sub>2</sub> expressed by crude segregation  
289 of quartzo-feldspathic and mafic minerals, or extreme elongation of feldspar  
290 grains in L-tectonites.

### 291 3.2.3 Low melt volume migmatites

292 Kilometre-scale bands of low melt volume stromatic or ophthalmic  
293 migmatites are commonly in faulted contact with quartz biotite mylonites. They  
294 are best developed on the RF close to the Myanmar border north of Ban Pak

295 Chan (Fig. 5), within the isolated ductile core north of Kapoe, and on the  
296 eastern side of Khao Phanom, the KMF ductile core (Fig. 7). The mesosome of  
297 these migmatites is compositionally similar to the mylonites, but foliation-  
298 parallel biotite is more coarse grained, and clots of fibrolitic sillimanite suggest  
299 that the migmatite is a higher grade development of the mylonite. A spaced  
300 schistosity is defined by biotite domains and quartzo-feldspathic microlithons.  
301 A fine biotite mineral lineation marks foliation surfaces.

302 Sigma-type quartz lenses are well developed within the mesosome, and  
303 contain significant amounts of K-feldspar and euhedral hornblende. These are  
304 compositionally similar to coarse microlithons, and indicate a progression from  
305 quartz-biotite segregation in the mylonites, to more complete mafic-felsic  
306 segregation and incipient melting. Larger leucosomes have the same  
307 composition, but are coarser, more feldspathic, and possess a variably  
308 developed foliation defined by hornblende and elongate quartz shape preferred  
309 orientation. They are also surrounded by dark, felsic depleted melanosomes,  
310 indicating local melt derivation. Fully developed leucosomes range in thickness  
311 from 1 cm to 2 m, and form sheet-like bodies parallel to  $S_2$ , but rarely comprise  
312 more than 20 % of the total rock volume. The contact between the two  
313 components is usually sharp, but locally diffuse.

314 In all cases the leucosomes are necked, and often form well-spaced  
315 ellipsoidal ductile boudins (Fig. 3e). Extensional shears with a dextral  
316 asymmetry form between boudins at angles less than  $30^\circ$  to the tectonic fabric;  
317 these are thus interpreted as synthetic shear bands. More rarely, boudins are

318 separated by antithetic shear bands with a sinistral shear sense. In both  
319 instances, the host foliation flows smoothly around the pinch and swell  
320 structures, and the shear bands curve into parallelism with the foliation  
321 immediately outside the leucosome. Since formation of the mesosome  
322 schistosity is interpreted to be coeval with  $D_2$  dextral shear, and leucosomes  
323 form parallel to this fabric and also record dextral deformation in the same  
324 orientation, it can be inferred that migmatization was syn-kinematic with  
325 respect to  $D_2$ .

#### 326 *3.2.4 Quartz-biotite mylonites*

327 Quartz-biotite mylonites form broad bands of fairly homogeneous  
328 deformation. They have a similar composition to the low melt volume  
329 migmatites, but all minerals are finer, the foliation is more continuous and  
330 microlithons are thin and composed entirely of quartz. Sillimanite and melt  
331 lenses are absent. Faint colour and compositional banding parallel to  $S_2$  may be  
332 the remnants of sedimentary bedding in the protolith, while lithic clasts of  
333 granite, quartzite and quartz flattened parallel to  $S_2$  and stretched parallel to the  
334 mineral lineation also attest to a sedimentary origin. Lithic clasts are present in  
335 a more deformed state in the low melt volume migmatite. Their size,  
336 composition and distribution in a bedded, fine grained silicic rock indicates that  
337 the protolith for both lithologies may be the pebbly mudstones of the Kaeng  
338 Krachan Group, which are found in an un-deformed state adjacent to both  
339 faults. Deposition of the Kaeng Krachan Group ended in the Lower Permian



340 (e.g. Bunopas et al., 1991; Fujikawa et al., 2005), placing a maximum age limit  
341 on the onset of  $D_2$ .

342 The long axes of deformed sedimentary clasts are rotated anti-  
343 clockwise relative to the foliation in horizontal section, forming a dextral stair-  
344 stepping geometry augmented by crystal-plastic quartz mantles. Similar sigma-  
345 type quartz objects without obvious cores form foliation-parallel asymmetric  
346 ductile boudin trails. These may be pre-metamorphism quartz veins rotated or  
347 transposed into parallelism with the foliation. However, grain sizes and sub-  
348 grain rotation patterns in the boudins are identical to grains in microlithons  
349 between biotite rich domains, indicating that they formed by the same  
350 processes, perhaps as a stage towards a more gneissic segregation. It is  
351 interesting to note that the vast majority of asymmetric objects are sigma-type;  
352 delta-type objects are rare, especially in the KMF. This may indicate low strain  
353 rates, as the embayments typical of delta-type objects can be filled by  
354 recrystallised material before the object has rotated further during low strain  
355 (Passchier and Simpson, 1986).

356 Other dextral shear sense indicators in both the mylonite and low melt  
357 migmatite include S-C' fabrics, mica fish and asymmetric folds. Folding during  
358  $D_2$  was less well developed than during  $D_1$ , but always had a ductile nature, and  
359 formed long amplitude, short wavelength structures with dextral vergence.  
360 Three broad fold styles are characteristic. The first is harmonic similar folding  
361 of  $S_2$  which is common in more homogeneous quartz-biotite mylonites. Axial  
362 planes are subparallel to  $S_2$ , and hinge lines appear to be orthogonal to the

363 ductile lineation. It is likely that these represent oblique sections through the  
364 noses of tubular sheath folds. Structurally similar folds affect high melt volume  
365 migmatites along Huai Chang Raek, SW of Bang Saphan Noi (Fig. 2 and Fig.  
366 6). These also have steeply plunging hinge lines, but their axial planes strike ~  
367 150°, oblique to the foliation and migmatitic segregation. Structures indicating  
368 high grade dextral shear flow around the folds, and leucosome bands are  
369 transposed into parallelism with fold axes, and into discontinuous bands  
370 striking ~050° where short limbs are highly thinned. These are interpreted to be  
371 late D<sub>2</sub> folds formed during retrograde metamorphism, and are synchronous  
372 with low grade S-C' fabrics in the foliated granites. The third fold style occurs  
373 in the low melt migmatites. Thin leucosomes can display disharmonic  
374 ptygmatic and rootless folds (Fig. 3f), and therefore indicate continued ductile  
375 deformation after melt segregation. All folds are coeval with D<sub>2</sub>.

### 376 3.3 D<sub>3</sub>

377 D<sub>3</sub> is characterised by a period of sinistral strike-slip faulting, marked at  
378 the surface by steeply dipping faults with a wide range of orientations, but  
379 dominantly between 000° and 030°. Most of the Thai Peninsula between Phuket  
380 and Pran Buri is intensely cut by an anastomosing network of these structures  
381 (Fig. 2). They occur both within and outside the D<sub>1</sub>-D<sub>2</sub> ductile cores, and within  
382 the central, most densely faulted region, divergent branches re-link to form  
383 elongate wedges containing metamorphic rocks in abrupt contact with  
384 unsheared sedimentary rocks. Steep, linear valleys and elongate karstic  
385 mountains are the characteristic geomorphic expression of these structures (Fig.

386 8a), so they can be traced from satellite imagery. A swathe of faults on the RF  
387 is 440 km long and up to 50 km wide, though individual strands are rarely  
388 longer than 150 km. Combined with a ~200 km projection offshore into the  
389 Mergui Basin (Intawong, 2006; Polachan, 1988), the total brittle length of the  
390 RF may be between 500 and 650 km. Onshore faults are concentrated on the  
391 Thai side of the border, with fewer, but longer and more deeply incised fault  
392 valleys in Myanmar. To the west of the main population, the strands start to  
393 curve to the north and NW, where they enter the Andaman Sea near Mergui.

394 The KMF has a much simpler expression, with only about six major  
395 strands, all of which have very clear topographic expression, defining a fault  
396 zone 210 km long and 25 km wide. A number of short, parallel faults exist  
397 within the relatively undeformed block between the RF and KMF, which has a  
398 width no more than 50 km normal to the structural trend. Fault density  
399 decreases towards the east of the peninsula on both faults, though it is possible  
400 that structures exist in this area and are hidden by Quaternary deposits. Strands  
401 at the northeastern end of both fault zones appear to curve northward before  
402 disappearing.

403 Outcrops of major fault strands are characterised by zones of cataclasis  
404 tens of metres wide, mostly composed of coarse, poorly sorted, angular clasts  
405 set in a matrix of finer breccia, unfoliated gouge or quartz (Fig. 8b). Within  
406 these zones, narrow, anastomosing bands of high strain contain fine breccia,  
407 foliated gouge and discrete fault planes with slickensides. Several generations

408 of high strain bands are often present within a single major  $D_3$  strand, which  
409 record a complex history of overprinting and reactivation.

410 Breccia zones between unshered sediments and high grade  
411 metamorphic rocks are made up of fragments of both lithologies, which are  
412 increasingly mixed and rotated away from their original orientation towards the  
413 centre of the breccia zone. Clast shapes include nested duplex-like stacks of  
414 orthorhombic slivers, and more equant fragments. Within at least two fault  
415 strands on the RF, unfoliated feldspar veins injected into an early fault breccia  
416 have cooled and subsequently been sliced into angular blocks themselves by  
417 narrow, chlorite-rich faults. A similar process may account for the more  
418 common quartz breccias composed of clasts of an older quartz breccia together  
419 with fragments of host rock. At the margin of breccia bands the host rock is  
420 often intensely fractured and veined, with small discrete faults in all  
421 orientations forming a broad damage zone.

422 Large, discrete fault planes exist both within the cataclasis zone of  
423 major brittle strands, and as isolated minor structures in intact rock. They are  
424 often polished and marked by slickensides which indicate either pure strike-  
425 slip, or oblique-slip movement. In the latter case, slickensides plunge up to  $50^\circ$   
426 to the NE or SW. More rarely, two or more generations of slickensides are  
427 present on the same plane, with the oldest almost always sub-horizontal. Fault  
428 plane steps are usually ambiguous, but tend to indicate sinistral motion, or  
429 reverse sinistral where they are oblique. Small contractional duplexes in oblique  
430 damage zones also indicate reverse oblique sinistral shear. Occasional normal

431 overprinting of the reverse sinistral fabrics indicates localised extension during  
432 the late stages of, or after, D<sub>3</sub> (Fig. 8c).

433         The contrast between neighbouring rocks on either side of D<sub>3</sub> faults is  
434 sometimes extreme. For example, the biotite-sillimanite low melt migmatites of  
435 the KMF exposed on the eastern side of Khao Phanom occur within 3.5 km of  
436 undeformed limestones of the Ratburi Group (Fig. 7). The actual contact is  
437 obscured by alluvium, and may be much closer. Contacts on the east side of the  
438 western RF D<sub>2</sub> strand NW of Chumphon are even more abrupt. High melt  
439 volume migmatites and amphibolite facies granite mylonites crop out within 50  
440 m of pebbly mudstones of the Kaeng Krachan Group and Jurassic red-beds  
441 (Fig. 5), neither of which shows any evidence of homogeneous strain, contact  
442 or regional metamorphism. This implies significant vertical movement. There is  
443 no evidence of large scale thrusting, and 83 % of 368 measured D<sub>3</sub> fault planes  
444 have dips  $\geq 45^\circ$ .

445         Absolute displacement of individual fault strands is usually unclear, as  
446 most lithological boundaries are parallel to the faults. Where there is obliquity,  
447 however, a minimum estimate can be made. For example, the Ranong granite is  
448 obliquely truncated by a dextral D<sub>2</sub> shear zone, but part of the deformed  
449 northern tip of the granite has a present-day sinistral offset relative to the main  
450 body of at least 10 km along three D<sub>3</sub> strands (Fig. 4). Displacements visible in  
451 the field are in the order of decimetres (Fig. 8d), proportional to the reduced  
452 width of the individual faults. The total displacement on the fault zones must be  
453 the sum of individual displacements on major strands. If the Ranong example is

454 typical, an average sinistral slip of about 3.3 km may characterise the main  
455 strands. The RF is composed of at least 25 major  $D_3$  strands, yielding an  
456 estimated displacement of about 80 km. The KMF has fewer strands, and  
457 displacement may be of the order of 20 km.

#### 458 *3.4 D<sub>4</sub>*

459 The least intense phase of deformation,  $D_4$  was a period of brittle dextral  
460 strike-slip faulting. It is expressed by outcrop scale strike-slip fault arrays  
461 which are pervasive across the KMF and RF, and cut across the metamorphic  
462 cores and  $D_3$  fault zones. The faults are typically discrete, planar surfaces less  
463 than 10 m long, and often just several centimetres long. Thin bands of gouge  
464 are developed only on the larger through-going faults. Features such as R (Fig.  
465 8e) and R' Riedel shears, P-shears, releasing bends and horsetail splays are well  
466 developed and typically indicate dominant dextral displacement (Fig. 9). These  
467 structures strike between  $050^\circ$  and  $120^\circ$ , and so are commonly at a high oblique  
468 angle to the older fabrics (Fig. 9). They have vertical to very steep dips.

469 Shear sense and amount are usually clear because of this obliquity.  
470 Markers such as migmatite leucosome bands and quartz segregations in  
471 mylonites are cleanly deflected, show little folding into the faults, and are not  
472 altered by fault fluids (Fig. 8f). Dextral displacement is typically 0.5 to 10 cm  
473 on individual faults, but can be an order of magnitude higher across well  
474 developed arrays. Antithetic sinistral faults are locally observed at about  $45^\circ$   
475 clockwise from the main array, though these are subordinate in length and  
476 displacement (Fig. 9). Mineral precipitation is limited to rare quartz crystals

477 which indicate strike-normal extension, perhaps during a later dilatational  
478 phase. In one region within the KMF ductile core, space generated by horsetail  
479 splays at the ends of  $D_4$  faults has been intruded by a quartzo-feldspathic fluid  
480 which may have a magmatic origin, and would be the youngest such intrusion  
481 in the fault zone.

482 Remote sensing data indicate that kilometre-scale faults with similar  
483 orientations cross cut the major sinistral faults, and very occasionally show  
484 topographic dextral displacements. It is possible that these are the main foci of  
485  $D_4$  strain, and the outcrop faults simply represent dissipation of this strain  
486 within fault-bounded blocks.

## 487 **4.0 Timing of fault activity and magmatism**

### 488 *4.1 Timing of $D_1$ and $D_2$*

489 While there are no isotopic age data from the mylonites and migmatites  
490 on either fault, a considerable number of dates exist in the literature for the  
491 granitoid plutons, stocks, dykes and associated pegmatites which lie along the  
492 faults' traces throughout the Thai Peninsula. Their petrology and  
493 geochronology have been extensively studied, principally because they host  
494 globally important reserves of tin (e.g. Bignell, 1972; Charusiri, 1989; Cobbing  
495 et al., 1986; Hutchison, 1989; Putthapiban and Schwartz, 1994; Schwartz et al.,  
496 1995). It is informative to put these data into the context of the KMF and RF  
497 deformation history presented here.

498           Where intrusions interact with the fault zones, they can be classified as  
499 pre-, syn-, or post-kinematic with respect to each deformation phase. No  
500 intrusions in the fault zones can be shown to be pre-kinematic with respect to  
501  $D_1$ , while only two are unequivocally pre-kinematic with respect to  $D_2$ , both on  
502 the RF. These are the Ranong (Fig. 4) and Khao Wang Tal (Fig. 6) granites,  
503 which are cut by major ductile shear zones, and a gradient is exposed across  
504 strike from the undeformed intrusion into the sheared rocks. In addition to these  
505 intrusions, brittle fault-bounded granites in the region of retrograde S-C' fabric  
506 development west of Tha Sae show inhomogeneous deformation, with narrow,  
507 S-fabric parallel high strain ultramylonite bands. Such a feature is characteristic  
508 of deformation of pre-kinematic material (Gapais, 1989).

509           The Ranong granite (Fig. 4) is of particular importance because of its  
510 clear cross-cutting relationships with  $D_1$  and  $D_2$ . A band of  $D_1$  sheared meta-  
511 sediments extends from east of Ban Pak Chan to Ko Son, SSW of Ranong. It is  
512 obliquely cut at about  $10^\circ 5' N$  by the Ranong granite, a 45 km long, N-S  
513 trending coarse grained porphyritic biotite  $\pm$  muscovite intrusion. Its euhedral  
514 K-feldspar phenocrysts have a fairly constant grain shape preferred orientation  
515 parallel to the intrusion's long axis, but there is no evidence of strike-slip  
516 motion during its emplacement. The NNE striking meta-sediment band  
517 continues undeflected across both sides of the intrusion, and its contact with the  
518 granite appears not to be faulted, supporting our interpretation that the Ranong  
519 Granite was intruded into the meta-sediments, and therefore post-dates  $D_1$ .



520           The northwestern end of the intrusion is abruptly truncated by an  
521 oblique 3.5 km wide ductile shear zone of granite mylonite and low melt  
522 volume migmatite, which extends offshore into the Mae Nam Kra Buri estuary /  
523 Andaman Sea. Both lithologies contain abundant dextral shear sense indicators  
524 as described in section 3.2. There is a steep, but apparently continuous  
525 deformation gradient from the undeformed pluton into the shear zone. Quartz  
526 develops progressively more bulging recrystallisation and chlorite is present,  
527 while further into the shear zone sub-grain rotation dominates and biotite is the  
528 principal phyllosilicate. Within the fully developed mylonites in the centre of  
529 the shear zone, quartz deforms by grain boundary migration, and feldspar  
530 begins to be recrystallised.

531           This shear zone is characteristic of the higher grade metamorphic fault  
532 rocks across the KMF and RF, and since it cuts the Ranong granite, which itself  
533 post-dates  $D_1$ , it is assigned to  $D_2$ . Charusiri (1989) used Ar-Ar  
534 thermochronology on mica separates to date emplacement of a leucogranite  
535 within the Ranong Granite, and Sn-W mineralisation outside the main intrusion.  
536 He concluded that these events occurred between 82 and 77 Ma. Although less  
537 reliable, Charusiri's (1989) reassessment of Bignell's (1972) whole rock Rb-Sr  
538 data for the undeformed parts of the Ranong Granite yields an age of 87 Ma,  
539 lending some support to a Late Cretaceous age to the body. This age means  $D_1$   
540 must have concluded by the mid Late Cretaceous, and  $D_2$  must have started  
541 after this time.

542 Bignell (1972) used the K-Ar method to date muscovite from a foliated  
543 biotite – muscovite granite at Ban Set Takuat (Fig. 4), within the D<sub>2</sub> shear zone  
544 which truncates the Ranong granite, to propose a cooling age of 68.1 Ma. It has  
545 been shown above that dextral shear ceased before the rocks cooled below the  
546 field of bulging dynamic recrystallisation for quartz (~ 300°C) (Stipp et al.,  
547 2002). Since the K-Ar closure temperature for muscovite is  $350 \pm 50$  °C  
548 (Hames and Bowring, 1994), Bignell's (1972) age can be interpreted as cooling  
549 after D<sub>2</sub> metamorphism, which was sufficiently hot to have reset older  
550 magmatic mica geochronometers. The K-Ar method is now regarded unreliable  
551 in such applications, but this is the only date from the metamorphic rocks of  
552 either fault zone. It is considerably younger than the inferred age of the granite,  
553 consistent with field relationships which indicate that the Ranong Granite is  
554 pre-kinematic with respect to D<sub>2</sub>.

555 Northwest of Bang Saphan Noi (Fig. 6), a NNE-trending unfoliated  
556 pegmatite dyke intruded into a sliver of rocks displaying characteristic D<sub>1</sub>  
557 fabrics yielded a muscovite Ar-Ar age of  $71.77 \pm 0.55$  Ma (Charusiri, 1989).  
558 This is interpreted to date the D<sub>1</sub>-D<sub>2</sub> inter-kinematic magmatism which includes  
559 the Ranong granite, and other undated intrusions which display the same field  
560 relationships.

561 In many cases, foliated granites and orthogneisses interpreted to have  
562 been deformed during D<sub>2</sub> are found only within the exhumed metamorphic  
563 cores, and so it is not clear whether they are pre- or syn-kinematic. D<sub>2</sub> across  
564 the KMF and RF represents a prolonged phase of metamorphism and

565 migmatization in one or more ductile shear zones which may penetrate to a  
566 considerable depth in the lithosphere. Magmatism commonly occurs in such  
567 settings because of the close link between conditions of tectonic deformation  
568 and granite melting (Druguet and Hutton, 1998; Hutton, 1992). Intraplate  
569 crustal-scale strike-slip faults which penetrate the lithospheric mantle can act as  
570 continuous melt conduits (Leloup et al., 1995), and focus magmatic generation,  
571 ascent and emplacement (Hutton, 1988; Hutton and Reavy, 1992). Examples of  
572 high strain shear zones which contain syn-kinematic intrusions include the  
573 TIPA shear zone, Argentina (Höckenreiner et al., 2003), the Main Donegal  
574 Shear Zone, Ireland, (Hutton, 1982), and the Closepet granite, southern India  
575 (Moyen et al., 2003). On this basis it might be expected that some of the  
576 foliated granites in the KMF and RF are syn-kinematic with respect to D<sub>2</sub>. The  
577 criteria of Searle (2006) can be used to help determine whether this is the case.

578

579 The following features indicate a syn-kinematic origin:

580

- 581 1.) Based on field evidence and remote sensing data, none of the sheared  
582 granites (with the exception of the Ranong and Khao Wang Tal  
583 granites) can be traced outside the ductile fault zones.
- 584 2.) Where a more complete ductile strand is exposed, for example the area  
585 around Khao Plai Khlong Hin Phao within the RF (Fig. 5), there is a  
586 gradient from sheared granite in the east, to high then low melt volume  
587 migmatite, then lower grade quartz-biotite mylonites in the west, despite

588 disruption from younger faults. A similar pattern occurs across the KMF  
589 ductile core (Fig. 7). Although this sequence is not exposed in all parts  
590 of the faults, high grade metamorphic rocks occur along the whole  
591 length of the exposed ductile cores. This indicates a close spatial and  
592 dynamic link between migmatisation, syn-tectonic intrusions and high  
593 grade metamorphism.

594 3.) *In situ* melting occurs in all of these areas, and all leucosomes are  
595 affected to a greater or lesser extent by shearing, with the development  
596 of foliations and mineral lineations. Shear sense and orientation are the  
597 same in both components of migmatites and in sheared granites.

598 4.) Migmatite xenoliths are common in the weakly foliated granite of the  
599 KMF ductile core.

600 5.) Large granitic bodies within the migmatite zone of the KMF ductile  
601 core display a notably broad spectrum of deformation intensity over a  
602 narrow area. Fabrics range from magmatic to sub-magmatic hornblende  
603 mica and feldspar lineations, to well developed metamorphic mica  
604 foliations and crystal-plastic feldspar deformation. This variation may  
605 reflect variable strain as a result of being emplaced at different times  
606 during D<sub>2</sub>.

607 6.) Late stage pegmatite dykes within foliated granites typically record  
608 lower levels of strain than their host rocks.

609

610           These criteria suggest that some of the foliated granites in the KMF and  
611 RF formed during  $D_2$ , possibly related to partial melting associated with  
612 formation of the western province granites. There are presently no age data  
613 from any of the foliated bodies.

614

615           Intrusive bodies which are post-kinematic with respect to  $D_2$  lie along  
616 the central section of the RF. A suite of irregularly shaped porphyritic biotite-  
617 muscovite granite intrusions west of Bang Saphan Noi lie wholly within a 5 km  
618 wide sliver of high melt volume migmatite (Fig. 6), but show no evidence of  
619 solid state ductile deformation. An equally undeformed intrusion along the high  
620 ridge of Khao Plai Khlong Hin Phao (Fig. 5), west of Tha Sae, is broadly  
621 parallel to the ductile fabric of the mylonites it intrudes, but its contacts locally  
622 cross cut it. Neither deflection of the ductile fabric, nor systematic variation in  
623 country rock composition and texture is observed as a function of proximity to  
624 the intrusions. The granite – country rock contact is locally faulted by narrow  
625 brittle faults and thin, low grade mylonite zones, but the primary contact is  
626 interpreted to be intrusive. Most critical to this interpretation is the presence of  
627 small xenoliths of granitic ultramylonite within the pluton. A large, irregularly  
628 shaped migmatite xenolith found within one of the plutons west of Bang  
629 Saphan Noi also supports the conclusion that these granites post-date  $D_2$   
630 deformation, and are not low strain enclaves of pre-kinematic basement  
631 surrounded by anastomosing high strain shear zones.

632           None of the bodies which intrude exposed D<sub>2</sub> metamorphic cores have  
633 been dated. However, a biotite separate from a medium grained biotite ±  
634 muscovite granite NW of Thap Sakae was dated by Charusiri (1989), using the  
635 Ar-Ar method, at  $53.24 \pm 0.71$  Ma; and by Bignell (1972) using the K-Ar  
636 method, also on a biotite separate, at 51.8 Ma. The intrusion is compositionally  
637 and texturally similar to nearby intrusions within the migmatites. If these bodies  
638 were emplaced at the same time, as part of the fault controlled early Eocene  
639 magmatism proposed by Charusiri (1989), they indicate that D<sub>2</sub> on the RF  
640 terminated before about 54 Ma.

641           The Khao Lak granite, 12 km west of the KMF ductile strand, is hosted  
642 mostly by Permo-Carboniferous siliciclastics, yet contains large xenoliths of  
643 migmatitic mylonite. This indicates that there are ductile fault rocks at depth  
644 which have not been exhumed, through which the granite passed during its  
645 ascent; and secondly, that the granite is post-kinematic with respect to D<sub>2</sub>.  
646 Charusiri (1989) determined a muscovite Ar-Ar total fusion age of  $55.65 \pm 0.49$   
647 Ma for pegmatites within this body. Near Nam Tok Bang Thao Mae, within the  
648 KMF ductile core (Fig. 7), muscovite from an undeformed pegmatite vein  
649 which cuts D<sub>2</sub> mylonitic foliation yields a clear Ar-Ar plateau age of  $41.32 \pm$   
650  $0.17$  Ma (Charusiri, 1989). These results confirm that Eocene post-D<sub>2</sub>  
651 magmatism affected the KMF as well as the RF, and that D<sub>2</sub> must have ended  
652 before latest Paleocene to early Eocene times (~ 56 to 52 Ma) on both faults.

653 *4.2 Timing of D<sub>3</sub> and D<sub>4</sub>*

654 It has been shown that metamorphic cores deformed by D<sub>1</sub> and D<sub>2</sub> are  
655 bounded, cut, and probably exhumed by D<sub>3</sub> brittle faults. The onset of D<sub>3</sub>  
656 therefore post-dates the latest Paleocene to early Eocene (~56 to 52 Ma)  
657 termination of D<sub>2</sub>. Brittle faults assigned to D<sub>3</sub> on the basis of their scale,  
658 orientation and topographic expression also cut all post D<sub>2</sub> granites (with the  
659 possible exception of the Bang Thao Mae pegmatite). In addition to the 56 to 52  
660 Ma ages for these rocks reviewed in section 4.1, a suite of I – and S – type  
661 granites in the Ko Phuket – Phang Nga area yield mica Ar-Ar ages of 58-55 Ma  
662 (late Paleocene to earliest Eocene) (Charusiri, 1989). Although they do not  
663 cross D<sub>1</sub>-D<sub>2</sub> structures, they are clearly deformed by at least two major D<sub>3</sub>  
664 faults, and several smaller brittle structures (Fig. 2). The consistent ages of  
665 granites pre-kinematic with respect to D<sub>3</sub> across the KMF and RF indicates that  
666 D<sub>3</sub> began after the early Eocene (~ 52 Ma).

667 The offshore tectonic record can help to reinforce the constraints on  
668 fault timing established above. Numerous Tertiary basins exist east of the  
669 peninsula (Gulf of Thailand) and to the west (Andaman Sea), together with a  
670 number of small onshore basins (Fig. 1 and Fig. 2). Their relationship to  
671 movement on the KMF and RF is widely disputed. Models which show the  
672 basins as pull-aparts between pairs of strike-slip faults include those of  
673 Polachan et al. (1991) and Tapponnier et al. (1982). These models invoke  
674 Himalayan lateral extrusion as the driving force behind the strike-slip faults.  
675 More recent models, including those of Westaway and Morley (2006) and Hall

676 and Morley (2004) propose rifting, lower crustal flow and plate edge forces as  
677 principal driving mechanisms, in which case the KMF and RF act as  
678 accommodation structures under regional extension (Intawong, 2006).

679 In the Gulf of Thailand, four main basins are formed by N-S trending  
680 grabens and half grabens (Polachan et al., 1991). From west to east, these are  
681 the Chumphon, Western, Kra and Pattani Basins, while the Cambodian Khmer  
682 Basin and the larger Malay Basin lie to the east and southeast respectively.  
683 Between 4 and 8 km of poorly dated terrestrial sediments fill these basins.  
684 Estimates of the ages of the oldest sediments vary from Eocene to Oligocene  
685 age, and the basins experienced subsidence rates almost an order of magnitude  
686 greater than rift basins in the North Sea, and have high present day heat flow  
687 (Hall and Morley, 2004).

688 A series of N-S trending grabens and half grabens form the Mergui  
689 Basin at the south western end of the RF. The fault forms the northern boundary  
690 of, and dies out west of the Ranong Trough, the eastern-most graben in the  
691 Mergui basin (Polachan, 1988). This is about 200 km along strike from where  
692 the RF passes offshore near Takua Pa. Up to 8 km of sediments fill the deepest  
693 parts of the basin, with syn-rift sedimentation beginning in the Late Oligocene  
694 (Polachan, 1988), Early Oligocene (Andreason et al., 1997), or Late Eocene  
695 (Mahattanachai, pers. comm., 2007).

696 Onshore, the N-S trending Khien Sa and Krabi Basins (Fig. 2) lie south  
697 of the KMF. Mammalian fossils, including primates, found in the lowest levels  
698 of the Krabi Basin indicate a Late Eocene age (Chaimanee et al., 1997), and



699 show that E-W extension on the Thai Peninsula was underway by 35 Ma  
700 (Ducrocq et al., 1995).

701 Whilst there is a close spatial relationship between the Tertiary basins  
702 and the KMF and RF, major through-going strike-slip faults are not prominent  
703 on seismic data east of the peninsula (Intawong, 2006; Morley, 2001, 2002), as  
704 might be expected if the basins were pull-aparts. Nor are they restricted to  
705 within hypothetical horsetail splays. The N-S orientation of all the graben  
706 bounding faults is, however, consistent with E-W extension, which could also  
707 result in sinistral deformation on the KMF and RF. It follows that D<sub>3</sub> is  
708 kinematically compatible with the late Eocene – Oligocene onset of syn-  
709 kinematic sedimentation in N-S trending basins. This age is in accordance with  
710 the middle Eocene maximum age for D<sub>3</sub> indicated by onshore granite  
711 thermochronology.

712 A period of uplift during the latest Oligocene – earliest Miocene in the  
713 Chumphon basin (Intawong, 2006) (Fig. 2) marks the end of the first, and major  
714 rift phase. It can be correlated to inversion and an unconformity in the Pattani  
715 Basin (Jardine, 1997), the Mergui Basin (Polachan et al., 1991), and to undated,  
716 but stratigraphically similar unconformities in the onshore Krabi and Khien Sa  
717 Basins (Intawong, 2006). This inversion may be linked to the dextral D<sub>4</sub> faults  
718 which overprint all other structures on the KMF and RF. These faults formed at  
719 a shallow level in the crust, which suggests that exhumation of the metamorphic  
720 rocks was nearing completion by the time they formed in the latest Oligocene.

## 721 **5.0 Discussion**

### 722 *5.1 The early formation of the KMF and RF*

723 The work presented here shows that  $D_1 - D_2$  ductile dextral deformation  
724 started before 87 Ma (late Cretaceous), the oldest date (Charusiri, 1989) from  
725 the Ranong Granite which cuts  $D_1$  rocks and is cut by  $D_2$  rocks. It ceased before  
726 56 to 52 Ma (latest Paleocene to early Eocene), the ages of the granite at Thap  
727 Sakae equivalent to those which intrude RF  $D_2$  migmatites, and the Khao Lak  
728 granite which contains xenoliths of KMF mylonites. All these intrusive bodies  
729 are also cut by the same  $D_3$  faults which bound, cut, and probably exhume  $D_1$ -  
730  $D_2$  rocks.

731 It has previously been assumed that the KMF and RF, acting as  
732 conjugate structures to the TPF and MPF in Northern Thailand, underwent  
733 ductile dextral shear in the late Eocene, followed by brittle sinistral shear in the  
734 Miocene, as a result of lateral extrusion accompanying the India – Eurasia  
735 collision (e.g. Lacassin et al., 1997; Tapponnier et al., 1986). However, the  
736 evidence presented here means that  $D_1 - D_2$ , the high strain ductile phase of  
737 movement on the faults, preceded the start of the India – Eurasia collision,  
738 estimates for which include 55 Ma (Klootwijk et al., 1992), 55 Ma to 40 Ma  
739 (Molnar and Tapponnier, 1975), 54 Ma to 50 Ma (Searle et al., 1997), and 34  
740 Ma (Aitchison et al., 2007).

741 Consequently, it is necessary to look elsewhere for the cause of this  
742 deformation. The TPF and MPF also have a long and complex history of  
743 deformation and exhumation, only part of which is related to India-Eurasia

744 collision (e.g. Morley, 2004, Morley et al., 2007). The cause of early KMF and  
745 RF deformation may also be responsible for an older history to the TPF and  
746 MPF.

#### 747 *5.1.1 An orogenic event in Northern Thailand*

748 The fault zones coincide with the southern margin of a broad band of  
749 late Cretaceous to Paleocene uplift and orogenesis in Northern Thailand,  
750 Eastern Myanmar and Laos (Morley, 2004) (Fig. 10). Monazite ages from  
751 metamorphic core complex gneisses at Doi Inthanon, part of the Chiang Mai –  
752 Lincang belt in northern Thailand, record peak metamorphism between  $84 \pm 2$   
753 Ma and  $72 \pm 1$  Ma (Dunning et al., 1995). To the west, the Mogok  
754 Metamorphic Belt in Myanmar is parallel to the Chiang-Mai – Lincang belt,  
755 and experienced a phase of high grade metamorphism which was complete by  
756  $59.9 \pm 0.9$  Ma (Searle et al., 2007). Apatite fission track ages from Northern  
757 Thailand indicate maximum burial or onset of uplift at between 70 to 50 Ma  
758 (Upton, 1999), while the Cretaceous to Eocene Western Province granites were  
759 intruded into this orogen, and their present-day distribution closely follows its  
760 position (e.g. Charusiri, 1989, Charusiri et al., 1993; Cobbing et al., 1986;  
761 Hutchison, 1989; Putthapiban and Schwartz, 1994; Ridd, 1978). Typically of S-  
762 type geochemistry, they indicate melting of sedimentary rocks in the crust  
763 during thickening (e.g. Charusiri et al., 1993; Zaw, 1990).

764 The complex network of strike-slip faults in Northern Thailand, which  
765 include the MPF and TPF, may have originated as part of a belt of Late  
766 Cretaceous to Paleocene transpression within the thickened crust (Morley,

767 2004). Whether or not it was conjugate to this early phase of strike-slip  
768 faulting, the dextral phase on the KMF and RF may have helped to  
769 accommodate the difference in shortening between the orogen in the north, and  
770 the un – thickened crust to the south (Fig. 10).

#### 771 *5.1.2 Possible causes of the orogenesis*

772 While there is a clear coincidence between the position and timing of  
773 this orogenic event and dextral shear on the KMF and RF, the cause of the  
774 orogenesis is not clear. The most obvious involves the speculated West Burma  
775 Block (Mitchell, 1981). In the reconstructions of Metcalfe (1991, 1996, 2006),  
776 the West Burma Block was considered to be a continental fragment which  
777 accreted to the western edge of Sibumasu during the Late Cretaceous after the  
778 closure of the Meso-Tethys. Neogene dextral shear on the Sagaing fault and the  
779 Sumatran Fault, and 460 km of extension in the Andaman Sea had yet to occur  
780 (e.g. Curray, 2005; Curray et al., 1979; Hall, 1996, 2002; Maung, 1987),  
781 meaning that the southern part of this block would have been emplaced in a  
782 NNE direction immediately west of the N-S trending KMF and RF. Such an  
783 arrangement is compatible with localised indenter tectonics and dextral shear on  
784 the faults during the Late Cretaceous (Fig. 10).

785 Although continental basement xenoliths have been found in volcanics  
786 under the eastern Central Basin, (Pivnik et al., 1998), there is little evidence that  
787 West Burma represents a large continental fragment. Mitchell (1993) interprets  
788 the andesites, basalts, ophiolites, serpentinites and cherts of West Burma to be  
789 an intra-oceanic arc thrust north-eastwards over the Eurasian margin as the

790 Mawgyi Nappe, geologically similar to and contemporaneous with the Woyla  
791 Nappe of West Sumatra. The Woyla arc was thrust north-eastwards over  
792 Western Sumatra during the mid to late Cretaceous (Cameron et al., 1980;  
793 Barber, 2000). A band of I-type granitoid intrusions from Aceh to  
794 Bandarlampung cut through the nappe and basement material, providing a  
795 minimum age of emplacement. These bodies yield K-Ar ages of 120 Ma to 75  
796 Ma (McCourt et al., 1996), and may be correlatives of the 106 Ma to 91 Ma  
797 granodiorites and tonalites which intrude the Mawgyi Nappe (Mitchell, 1993).  
798 Although nappe emplacement would also have been associated with NNE-  
799 directed compression to the west of the KMF and RF, the ages of post-  
800 emplacement granites significantly pre-date the Northern Thailand orogenesis  
801 and D<sub>2</sub> deformation on the KMF and RF.

### 802 *5.1.3 Subduction variation along the Sunda Trench*

803         During the late Cretaceous, the Ceno-Tethys was being subducted  
804 northwards as India separated from Gondwana (Metcalf, 1996; Ramana et al.,  
805 1994). Between 73 and 57 Ma, India moved rapidly northward at about  
806 21cm/yr (Aitchison et al., 2007). However, while India progressed swiftly,  
807 Australia separated from Gondwana at a very slow rate (Besse and Courtillot,  
808 1991; Cande and Mutter, 1982). An oceanic spreading centre dominated by  
809 dextral transform zones may have existed between about 90 and 100 °E to  
810 accommodate the differences between these regions. To its west, subduction  
811 around the Sundaland margin was active, while the trench to its east was  
812 inactive (Hall 2008, *In Press*).

813           There is evidence in the deep mantle tomographic model of Bijwaard et  
814 al. (1998) of such a change in subduction. A pronounced change in structure  
815 east of 95-100°E at depths below 700 km marks the termination of cold, NW-  
816 SE trending linear anomalies, interpreted by van der Voo et al. (1999) to  
817 represent subducted Tethyan oceans. East of about 100°E, these anomalies are  
818 not present. This indicates that from Late Cretaceous times, Ceno-Tethys was  
819 subducted in the Sunda Trench west of 95°E only (Hall et al., 2007).

820           The KMF and RF lie in the over-riding plate along the projected path of  
821 the spreading centre and transform zone between these regions (Fig. 10). Given  
822 that the timing of D<sub>2</sub> proposed here coincides with the end of Mesozoic  
823 subduction east of 100°E, it is possible that dextral shear stresses at the edge of  
824 the subducting slab were transferred upwards into the continental margin.

## 825 *5.2 Brittle reactivation*

### 826 *5.2.1 Strike-slip inversion and exhumation of the ductile cores*

827           It has been shown that the metamorphic cores exposed at the surface  
828 along the KMF and RF lie in the centre of a complex, bifurcating network of  
829 brittle D<sub>3</sub> faults (Fig. 2). These thick zones of intense cataclasis record  
830 dominantly strike-slip, but also significant subordinate oblique-slip shear, and  
831 bring elongate slivers of metamorphic rocks of up to amphibolite facies into  
832 contact with unmetamorphosed sediments. Some adjacent D<sub>1</sub>-D<sub>2</sub> cores contain  
833 similar rocks, formed under similar metamorphic conditions, separated by  
834 brittle fault-bounded slivers of sedimentary cover. High to low strain gradients  
835 are only occasionally observed in individual cores, and regular, sinusoidal

836 curvature of the ductile foliation is not present, as might be expected if the  
837 cores represented individual ductile strands. Instead, the cores are interpreted  
838 simply as slices gouged out of one or more larger ductile shear zones, much of  
839 which may remain at depth, and therefore the slices do not represent the  
840 original D<sub>1</sub>-D<sub>2</sub> shear zone structure. In the absence of evidence for significant  
841 thrusting, it seems likely that differential uplift on such a scale must have  
842 occurred within D<sub>3</sub> positive flower structures along the central part of both  
843 faults (Fig. 11). Apatite fission-track ages from the Thai Peninsula indicate a  
844 period of exhumation between 44 Ma and 20 Ma, with the majority around the  
845 Oligocene – Miocene boundary (Upton, 1999). At this time D<sub>3</sub> was drawing to  
846 a close, and the fission track ages may represent denudation of a topography  
847 elevated by the flower structures.

848         The present day fault zones are therefore a *mélange* of slivers from all  
849 depths, which have been translated both vertically and longitudinally by D<sub>3</sub>  
850 faulting. Broad uplift associated with these structures may explain the elevated  
851 topography north of the KMF and throughout the RF, and the dramatic  
852 lithological change south of the KMF.

### 853 *5.2.2 Driving forces behind brittle reactivation*

854         The age of D<sub>3</sub> interpreted here corresponds closely to the re-initiation of  
855 subduction on the southern part of the Sunda Trench in the Middle Eocene,  
856 marked by arc volcanism in the Southern Mountains of East Java (Smyth,  
857 2005), and triggered by the acceleration in northward movement of Australia in  
858 the Early to Middle Eocene (Cande and Mutter, 1982; Royer and Sandwell,

1989). The oldest syn-rift sediments in many of the Tertiary basins across Sundaland were also deposited from the Middle to Late Eocene (summarised in Hall and Morley, 2004). These basins may have formed under a broad E-W extensional regime as a result of a N-S maximum horizontal stress, before active northwards subduction resumed ahead of Australia (Hall 2008, *In Press*). Thin, weak Sundaland lithosphere (Hall and Morley, 2004; Hyndman et al., 2005) rifted easily under these conditions, which were also compatible with sinistral movement on the NNE trending KMF and RF, weakened following D<sub>1</sub>-D<sub>2</sub> deformation and pre-, syn- and post kinematic magmatism. It therefore seems likely that the main brittle phase of faulting was triggered by the onset of Eocene-Recent subduction zone at the southern margin of Sundaland attempted to re-activate.

## 6.0 Conclusions

New field data combined with existing isotopic ages for the Western Province granites in peninsular Thailand allow a tentative kinematic history for the KMF and RF to be constructed:

- The KMF and RF are zones of major strike-slip faulting divided into four phases:
  - D<sub>1</sub> low grade ductile dextral strike-slip shear complete before 87 Ma.
  - D<sub>2</sub> medium to high grade ductile dextral strike-slip shear after 72 Ma and before 56 Ma.



- 882 D<sub>3</sub> brittle sinistral and sinistral reverse oblique strike-slip shear  
883 after 52 Ma.
- 884 D<sub>4</sub> brittle dextral strike-slip shear at about 23 Ma.
- 885 • Ductile dextral shear pre-dates both the India – Eurasia collision and  
886 ductile sinistral shear on the MPF and TPF, to which the KMF and RF  
887 had been assumed to be conjugate.
  - 888 • They may instead have accommodated the southern margin of a band of  
889 orogenesis in western Sundaland, which may be linked to cessation of  
890 subduction southeast of the northern tip of Sumatra in the Late  
891 Cretaceous.
  - 892 • Eocene – Oligocene D<sub>3</sub> reactivation of the fault zones during regional  
893 extension under a broadly N-S maximum principal stress was coeval  
894 with basin development offshore, and the resumption of subduction  
895 around the south of Sundaland.
  - 896 • Onshore transpression during D<sub>3</sub> resulted in deep rooted positive flower  
897 structures which exhumed slivers of the metamorphic shear zone.
  - 898 • Early Miocene inversion, particularly in the Tertiary basins nearest the  
899 faults, may be linked to D<sub>4</sub> strike-slip faulting across the fault zones.

900

## 901 **Acknowledgements**

902 We are grateful to the Department of Geological Sciences at Chiang Mai  
903 University and the Department of Mineral Resources, Bangkok, for their  
904 assistance and logistical support in the field; and to C.K. Morley for his

905 constructive review of the manuscript. This work is funded by the SE Asia  
906 Research Group at Royal Holloway, University of London, supported by a  
907 consortium of oil companies.  
908

ACCEPTED MANUSCRIPT

909 **References**

- 910 Aitchison, J.C., Ali, J.R., and Davis, A.M., 2007. When and where did India and Asia  
911 collide?. *Journal of Geophysical Research* 112, B05423,  
912 doi:10.1029/2006JB004706.
- 913 Andreason, M.W., Mudford, B., Onge, J.E.S., 1997. Geologic evolution and petroleum  
914 system of Thailand Andaman Sea Basins. In: Howes, J.V.C., Noble, R.A., (Eds.),  
915 Proceedings of the International Conference on Petroleum Systems of SE Asia  
916 and Australia, Indonesian Petroleum Association. pp. 337-350.
- 917 Baird, A., and Bosence, D., 1993. The sedimentological and diagenetic evolution of the  
918 Ratburi Limestone, Peninsular Thailand. *Journal of Southeast Asian Earth  
919 Sciences* 8, 173-180.
- 920 Barber, A.J., 2000. The origin of the Woyla Terranes in Sumatra and the Late Mesozoic  
921 evolution of the Sundaland margin. *Journal of Asian Earth Sciences* 18, 713-738.
- 922 Besse, J. and Courtillot, V., 1991. Revised and synthetic polar wander maps of the  
923 African, Eurasian, North American and Indian Plates, and true polar wander since  
924 200 Ma. *Journal of Geophysical Research* 96, 4029-4050.
- 925 Bignell, J.D., 1972. The geochronology of the Malayan Granites. Unpublished PhD  
926 Thesis, University of Oxford, 154 pp.
- 927 Bijwaard, H., Spakman, W., and Engdahl, E.R., 1998. Closing the gap between regional  
928 and global travel time tomography. *Journal of Geophysical Research* 103, 30055-  
929 30078.
- 930 Briaies, A., Patriat, P., and Tapponnier, P., 1993. Updated interpretation of magnetic  
931 anomalies and seafloor spreading stages in the South China Sea: Implications for

- 932 the Tertiary tectonics of Southeast Asia. *Journal of Geophysical Research* 98,  
933 6299-6328.
- 934 Bunopas, S., Jungyusuk, N., and Khositantont, 1991. Summary of geology of Southern  
935 Thailand. In: *Southern Thailand: Lithophile mineral deposits (Ranong – Takua Pa  
936 – Phuket)*, The Seventh Regional Conference on Geology, Mineral and Energy  
937 Resources of Southeast Asia and The Third Symposium IGCP 282: Rare Metal  
938 Granitoids. Geological excursion guidebook no.2, by Nakapadungrat, S.,  
939 Jungyusuk, N., Putthapiban, P., Kosuwan, S., and Chaimanee, N, 1-13.
- 940 Cameron, N.R., Clarke, M.C.G., Aldiss, D.T., Aspden, J.A., Djunuddin, A., 1980. The  
941 geological evolution of North Sumatra. In: *Proceedings of the Indonesian  
942 Petroleum Association, Annual Convention, 9*, pp. 149– 187.
- 943 Cande, S.C., and Mutter, J.C., 1982. A revised identification of the oldest sea-floor  
944 spreading anomalies between Australia and Antarctica. *Earth and Planetary  
945 Science Letters* 58, 151-160.
- 946 Chaimanee, Y., Suteethorn, V., Jaeger, J-J., and Ducrocq, S., 1997. A Late Eocene  
947 anthropoid primate from Thailand. *Nature* 385, 429-431.
- 948 Chârusiri, P., 1989. *Lithophile Metallogenetic Epochs of Thailand: A Geological and  
949 Geochronological Investigation*. Unpublished PhD Thesis, Queen’s University,  
950 Kingston, Ontario, Canada, 819 pp.
- 951 Chârusiri, P., Clark, A.H., Farrar, E., Archibald, D., and Chârusiri, B., 1993. Granite belts  
952 in Thailand: evidence from the  $^{40}\text{Ar}/^{39}\text{Ar}$  geochronological and geological  
953 syntheses. *Journal of Southeast Asian Earth Sciences* 8, 127-136.

- 954 Cobbing, E.J., Mallick, D.I.J., Pitfield, P.E.J., and Teoh, L.H., 1986. The granites of the  
955 Southeast Asian Tin Belt. *Journal of the Geological Society, London* 143, 537-  
956 550.
- 957 Curray, J.R., Moore, D.G., Lawver, L.A., Emmel, F.J., Raitt, R.W., Henry, M.,  
958 Kieckhefer, R., 1979. Tectonics of the Andaman Sea and Burma. In: Watkins,  
959 J.S., Montadert, L., Dickenson, P.W. (Eds.), *Geological and Geophysical*  
960 *Investigations of Continental Margins*, American Association of Petroleum  
961 Geologists, Memoir 29, pp. 189–198.
- 962 Curray, J.R., 2005. Tectonics and History of the Andaman Sea region. *Journal of Asian*  
963 *Earth Sciences* 25, 187-232.
- 964 Department of Mineral Resources, 1980. Geological map of Thailand, scale 1:50,000.
- 965 Department of Mineral Resources, 1982. Geological map of Thailand, scale 1:250,000.
- 966 Department of Mineral Resources, 1992. Geological map of Thailand, scale 1:50,000.
- 967 Department of Mineral Resources, 2006. Geological map of Thailand, scale 1:50,000.
- 968 Druguet, E., and Hutton, D.H.W., 1998. Syntectonic magmatism in a mid-crustal  
969 transpressional shear zone: an example from the Hercynian rocks of the eastern  
970 Pyrenees. *Journal of Structural Geology* 20, 905-916.
- 971 Ducrocq, S., Chaimanee, Y., Suteethorn, V., and Jaeger, J-J., 1995. Mammalian faunas  
972 and the ages of the continental Tertiary fossiliferous localities from Thailand.  
973 *Journal of Southeast Asian Earth Sciences* 12, 65-78.
- 974

- 975 Dunning, G.R., Macdonald, A.S., and Barr, S.M., 1995. Zircon and Monazite U-Pb  
976 dating of the Doi Inthanon core complex, northern Thailand: implications for  
977 extension within the Indosinian Orogen. *Tectonophysics* 251, 197-213.
- 978 England, P., and Houseman, G., 1986. Finite strain calculations of continental  
979 deformation 2. Comparison with the India-Asia collision zone. *Journal of*  
980 *Geophysical Research* 91, 3664-3676.
- 981 Fujikawa, M., Ueno, K., Sardud, A., Saengsrichan, W., Kamata, Y., and Hisada, K-i.,  
982 2005. Early Permian ammonoids from the Kaeng Krachan Group of the  
983 Phatthalung-Hat Yai area, southern peninsular Thailand. *Journal of Asian Earth*  
984 *Sciences* 24, 739-752.
- 985 Gapais, D., 1989. Shear structures within deformed granites: mechanical and thermal  
986 indicators. *Geology* 17, 1144-1147.
- 987 Garson, M.S., Young, B., Mitchell, A.H.G., and Tait, B.A.R., 1975. The geology of the  
988 tin belt in Peninsular Thailand around Phuket, Phangnga, and Takua Pa. *Overseas*  
989 *Memoir of the Institute of Geological Sciences*, 1, 112 pp.
- 990 Garson, M.S., and Mitchell, A.H., 1970. Transform faulting in the Thai Peninsula. *Nature*  
991 22, 45-47.
- 992 Gilley, L.D., Harrison, T.M., Leloup, P.H., Ryerson, F.J., Lovera, O.M., and Wang, J-H.,  
993 2003. Direct dating of left-lateral deformation along the Red River shear zone,  
994 China and Vietnam. *Journal of Geophysical Research* 108, 2127-2148.
- 995 Hall, R., 1996. Reconstructing Cenozoic SE Asia. In: Hall, R., and Blundell, D., (Eds),  
996 *Tectonic Evolution of Southeast Asia*, Geological Society Special Publication  
997 106, 153-184.

- 998 Hall, R., 2002. Cenozoic geological and plate tectonic evolution of SE Asia and the SW  
999 Pacific: computer-based reconstructions, model and animations. *Journal of Asian*  
1000 *Earth Sciences* 20, 353-431.
- 1001 Hall, R., and Morley, C.K., 2004. Sundaland Basins, Continent-Ocean Interactions  
1002 Within East Asian Marginal Seas. *Geophysical Monograph Series* 149, 55-85.
- 1003 Hall, R., van Hattum, M.W.A., Spakman, W., 2007. Impact of India-Asia collision on SE  
1004 Asia: The record in Borneo. *Tectonophysics*, In Press.
- 1005 Hames, W.E., and Bowring, S.A., 1994. An empirical evaluation of the argon diffusion  
1006 geometry in muscovite. *Earth and Planetary Science Letters* 124, 161-169.
- 1007 Höckenreiner, M., Söllner, F., and Miller, H., 2003. Dating the TIPA shear zone: an Early  
1008 Devonian terrane Boundary between the Famatinian and Pampean systems (NW  
1009 Argentina). *Journal of South American Earth Sciences* 16, 45-66.
- 1010 Hutchison, C.S., 1989. *Geological Evolution of South – East Asia*. Oxford Monographs  
1011 on Geology and Geophysics, Oxford University Press, Oxford, UK, 368 pp.
- 1012 Hutton, D.H.W., 1982. A tectonic model for the emplacement of the Main Donegal  
1013 Granite, NW Ireland. *Journal of the Geological Society, London* 139, 615-631.
- 1014 Hutton, D.H.W., 1988. Granite emplacement and tectonic controls: inferences from  
1015 deformation studies. *Transactions of the Royal Society of Edinburgh Earth*  
1016 *Sciences* 79, 245-255.
- 1017 Hutton, D.H.W., 1992. Granite sheeted complexes: evidence for the dyking ascent  
1018 mechanism. *Transactions of the Royal Society of Edinburgh: Earth Sciences* 83,  
1019 377-382.

- 1020 Hutton, D.H.W., and Reavy, R.J., 1992. Strike-slip tectonics and granite petrogenesis.  
1021 Tectonics 11, 960-967.
- 1022 Hyndman, R.D., Currie, C.A., Mazzotti, S., 2005. Subduction zone backarcs, mobile  
1023 belts, and orogenic heat. GSA Today 15, 4-9.
- 1024 Intawong, A., 2006. The structural evolution of Tertiary sedimentary basins in Southern  
1025 Thailand and their relationship to the Khlong Marui Fault. Unpublished PhD  
1026 thesis, Royal Holloway, University of London, UK
- 1027 Jardine, E., 1997. Dual petroleum governing the prolific Pattani Basin, Offshore  
1028 Thailand. Proceeding of International Conference on Stratigraphy and Tectonic  
1029 Evolution of Southeast Asia and the South Pacific, Bangkok, Thailand, 525-534.
- 1030 Klootwijk, C.T., Gee, J.S., Peirce, J.W., Smith, G.M., and McFadden, P.L., 1992. An  
1031 early India-Asia contact; palaeomagnetic constraints from Ninetyeast Ridge, ODP  
1032 Leg 121; with Suppl. Data 92-15. Geology 20, 395-398.
- 1033 Kornsawan, A., and Morley, C.K., 2002. The origin and evolution of complex transfer  
1034 zones (graben shifts) in conjugate fault systems around the Funan Field, Pattani  
1035 Basin, Gulf of Thailand. Journal of Structural Geology 24, 435-449.
- 1036 Lacassin, R., Maluski, H., Leloup, P.H., Tapponnier, P., Hinthong, C., Siribhakdi, K.,  
1037 Chuaviroj, S., and Charoenravat, A., 1997. Tertiary diachronic extrusion and  
1038 deformation of western Indochina: Structural and  $^{40}\text{Ar}/^{39}\text{Ar}$  evidence from NW  
1039 Thailand. Journal of Geophysical Research 102, 10,013-10,037.
- 1040 Lee, T-Y., and Lawver, L.A., 1995. Cenozoic Plate reconstruction of Southeast Asia.  
1041 Tectonophysics 251, 85-138.



- 1042 Leloup, P.H., Arnaud, N., Lacassin, R., Kienast, J.R., Harrison, T.M., Phan Trong, T.T.,  
1043 Replumaz, A., and Tapponnier, P., 2001. New constraints on the structure,  
1044 thermochronology, and timing of the Ailao Shan-Red River shear zone, SE Asia.  
1045 *Journal of Geophysical Research* 106, 6683-6732.
- 1046 Leloup, P.H., Lacassin, R., Tapponnier, P., Schärer, U., Dalai, Z., Xiaohan, L.,  
1047 Liangshang, Z., Shaocheng, J., and Trinh, P.T., 1995. The Aliao Shan-Red River  
1048 shear zone (Yunnan, China), Tertiary transform boundary of Indochina.  
1049 *Tectonophysics* 251, 3-84.
- 1050 Lepvrier, C., Maluski, H., Van Tich, V., Leyroloup, A., Thi, P.T., and Vuong, N.V.,  
1051 2004. The Early Triassic Indosinian orogeny in Vietnam (Truong Son Belt and  
1052 Kontum Massif); implications for the geodynamic evolution of Indochina.  
1053 *Tectonophysics* 393, 87-118.
- 1054 Maung, H., 1987. Transcurrent movements in the Burma – Andaman sea region. *Geology*  
1055 15, 911-912.
- 1056 McCourt, W.J., Crow, M.J., Cobbing, E.J., and Amin, T.C., 1996. Mesozoic and  
1057 Cenozoic plutonic evolution of SE Asia: evidence from Sumatra, Indonesia. In:  
1058 Hall, R., and Blundell, D., (Eds), *Tectonic Evolution of Southeast Asia*,  
1059 Geological Society Special Publication 106, 321-335.
- 1060 Metcalfe, I., 1991. Late Palaeozoic and Mesozoic palaeogeography of Southeast Asia.  
1061 *Palaeogeography, Palaeoclimatology, Palaeoecology* 87, 211-221.
- 1062 Metcalfe, I., 1996. Pre – Cretaceous evolution of SE Asian terranes. In: Hall, R., and  
1063 Blundell, D., (Eds), *Tectonic Evolution of Southeast Asia*, Geological Society  
1064 Special Publication 106, 97-122.

- 1065 Metcalfe, I., 2002. Permian tectonic framework and palaeogeography of SE Asia. *Journal*  
1066 *of Asian Earth Sciences* 20, 551-566.
- 1067 Metcalfe, I., 2006. Palaeozoic and Mesozoic tectonic evolution and palaeogeography of  
1068 East Asian crustal fragments: The Korean Peninsula in context. *Gondwana*  
1069 *Research* 9, 24-46.
- 1070 Mitchell, A.H.G., 1981. Phanerozoic plate boundaries in mainland SE Asia, the  
1071 Himalayas and Tibet. *Journal of the Geological Society of London* 138, 109-122.
- 1072 Mitchell, A.H.G., 1993. Cretaceous – Cenozoic tectonic events in the western Myanmar  
1073 (Burma) – Assam region. *Journal of the Geological Society, London* 150, 1089-  
1074 1102.
- 1075 Mitchell, A.H.G., Htay, M.T., Htun, K.M., Win, M.N., Oo, T., and Hlaing, T., 2007.  
1076 Rock relationships in the Mogok metamorphic belt, Tatkon to Mandalay, central  
1077 Myanmar. *Journal of Asian Earth Sciences* 29, 891-910.
- 1078 Molnar, P., and Tapponnier, P., 1975. Cenozoic tectonics of Asia: effects of a continental  
1079 collision. *Science* 189, 419-426.
- 1080 Morley, C.K., 2001. Combined escape tectonics and subduction rollback-back arc  
1081 extension: a model for the evolution of Tertiary rift basins in Thailand, Malaysia  
1082 and Laos. *Journal of the Geological Society, London* 158, 461-474.
- 1083 Morley, C.K., 2002. A tectonic model for the Tertiary evolution of strike-slip faults and  
1084 rift basins in SE Asia. *Tectonophysics* 347, 189-215.
- 1085
- 1086 Morley, C.K., 2004. Nested strike-slip duplexes, and other evidence for Late Cretaceous-  
1087 Palaeogene transpressional tectonics before and during India-Eurasia collision, in

- 1088 Thailand, Myanmar and Malaysia. *Journal of the Geological Society*, London  
1089 161, 799-812.
- 1090 Morley, C.K., and Westaway, R., 2006. Subsidence in the super-deep Pattani and Malay  
1091 basins of Southeast Asia: a coupled model incorporating lower-crustal flow in  
1092 response to post-rift sediment loading. *Basin Research* 18, 51-84.
- 1093 Morley, C.K., Smith, M., Carter, A., Charusiri, P., and Chantraprasert, S., 2007.  
1094 Evolution of deformation styles at a major restraining bend, constraints from  
1095 cooling histories, Mae Ping fault zone, western Thailand. In: Cunningham, W.D.,  
1096 and Mann, P., (eds), *Tectonics of Strike-Slip Restraining and Releasing Bends*,  
1097 Geological Society, London, Special Publications 290, 325-349.
- 1098 Moyen, J.-F., Nédélec, A., Martin, H., Jayananda, M., 2003. Syntectonic granite  
1099 emplacement at different structural levels: the Closepet granite, South India.  
1100 *Journal of Structural Geology* 25, 611-631.
- 1101 Nakapadungrat, S., Jungyusuk, N., Putthapiban, P., Kosuwan, S., and Chaimanee, N.,  
1102 1991. Southern Thailand: Lithophile mineral deposits (Ranong – Takua Pa –  
1103 Phuket). *The Seventh Regional Conference on Geology, Mineral and Energy*  
1104 *Resources of Southeast Asia and The Third Symposium IGCP 282: Rare Metal*  
1105 *Granitoids*. Geological excursion guidebook no.2, 76 pp.
- 1106 Packham, G.H., 1993. Plate tectonics and the development of sedimentary basins of the  
1107 dextral regime in western Southeast Asia. *Journal of Southeast Asian Earth*  
1108 *Sciences* 8, 497-511.
- 1109 Passchier, C.W., and Simpson, C., 1986. Porphyroclast systems as kinematic indicators.  
1110 *Journal of Structural Geology* 8, 831-843.

- 1111 Passchier, C.W., and Trouw, R.A.J., 2005. *Microtectonics*, 2<sup>nd</sup> Edition. Springer-Verlag,  
1112 Germany, 366pp.
- 1113 Pigott, J.D., and Sattayarak, N., 1993. Aspects of sedimentary basin evolution assessed  
1114 through tectonic subsidence analysis. Example: northern Gulf of Thailand.  
1115 *Journal of Southeast Asian Earth Sciences* 8, 407-420.
- 1116 Pivnik, D.A., Nahm, J., Tucker, R.S., Smith, G.O., Nyein, K., Nyunt, M., Maung, P.H.,  
1117 1998. Polyphase deformation in a fore-arc/back-arc basin, Salin subbasin,  
1118 Myanmar (Burma), *American Association of Petroleum Geologists Bulletin* 82,  
1119 1837-1856.
- 1120 Polachan, S., 1988. *The Geological Evolution of the Mergui Basin, S.E. Andaman Sea,*  
1121 *Thailand. Unpublished PhD Thesis, Royal Holloway and Bedford New College,*  
1122 *University of London, 218 pp.*
- 1123 Polachan, S., Praditdan, S., Tongtaow, C., Janmaha, S., Intarawijitr, K., and Sangsuwan,  
1124 C., 1991. Development of Cenozoic basins in Thailand. *Marine and Petroleum*  
1125 *Geology* 8, 84-97.
- 1126 Putthapiban, P., 1992. The Cretaceous – Tertiary granite magmatism in the west coast of  
1127 peninsular Thailand and the Mergui Archipelago of Myanmar/Burma. National  
1128 Conference on “Geological Resources of Thailand: Potential for Future  
1129 Development”, Department of Mineral resources, Bangkok, Thailand, 75-88.
- 1130 Putthapiban, P., and Schwartz, M.O., 1994. Geochronology of the Southeast Asian tin  
1131 belt granitoids. In: Seltmann, Kämpf and Möller (eds), *Metallogeny of Collisional*  
1132 *Orogens*, Czech Geological Survey, Prague, 391-398.

- 1133 Ramana, M.V., Nair, R.R., Sarma, K.V.L.N.S., Ramprasad, T., Krishna, K.S.,  
1134 Subrahmanyam, V., D'Cruz, M., Subrahmanyam, C., Paul, J., Subrahmanyam,  
1135 A.S., and Chandra Sekhar, D.V., 1994. Mesozoic anomalies in the Bay of Bengal.  
1136 Earth and Planetary Science Letters 121, 469-475.
- 1137 Rangin, C., Klein, M., Roques, D., Le Pichon, X, and Van Trong, L., 1995. The Red  
1138 River fault system in the Tonkin Gulf, Vietnam. Tectonophysics 243, 209-222.
- 1139 Replumaz, A., and Tapponnier, P., 2003. Reconstruction of the deformed collision zone  
1140 between India and Asia by backward motion of lithospheric blocks. Journal of  
1141 Geophysical Research 108, ETG 1-1 – 1-24.
- 1142 Ridd, M.F., 1978. Thailand. In: Moulladem, M., and Nairn, A.E.M., (eds.), The  
1143 Phanerozoic Geology of the World, II, The Mesozoic, A., Elsevier, Amsterdam,  
1144 145-163.
- 1145 Royer, J.Y., and Sandwell, D.T., 1989. Evolution of the Eastern Indian Ocean since the  
1146 Late Cretaceous; constraints from Geosat Altimetry. Journal of Geophysical  
1147 Research 94B, 13755-13782.
- 1148 Schwartz, M.O., Rajah, S.S., Askury, A.K., Putthapiban, P., and Djaswadi, S., 1995. The  
1149 Southeast Asian Tin Belt. Earth-Science Reviews 38, 95-293.
- 1150 Searle, M., Corfield, R.I., Stephenson, B., and McCarron, J., 1997. Structure of the North  
1151 Indian continental margin in the Ladakh-Zaskar Himalayas: implications for the  
1152 timing of obduction of the Spontang ophiolite, India-Asia collision and  
1153 deformation events in the Himalaya. Geological Magazine 134, 297-316.

- 1154 Searle, M.P., 2006. Role of the Red River Shear zone, Yunnan and Vietnam, in the  
1155 continental extrusion of SE Asia. *Journal of the Geological Society, London* 163,  
1156 1025-1036.
- 1157 Searle, M.P., Noble, S.R., Cottle, D.J., Waters, D.J., Mitchell, A.H.G., Hlaing, T., and  
1158 Horstwood, M.S.A., 2007. Tectonic evolution of the Mogok metamorphic belt,  
1159 Burma (Myanmar) constrained by U-Th-Pb dating of metamorphic and magmatic  
1160 rocks. *Tectonics* 26, TC3014.
- 1161 Smyth, H., 2005. Eocene to Miocene basin history and volcanic activity in East Java,  
1162 Indonesia. Unpublished PhD Thesis, Royal Holloway, University of London, 476  
1163 pp.
- 1164 Smyth, H., Hamilton, P.J., Hall, R., and Kinny, P.D., 2007. The deep crust beneath island  
1165 arcs: Inherited zircons reveal a Gondwana continental fragment beneath East  
1166 Java, Indonesia. *Earth and Planetary Science Letters* 258, 269-282.
- 1167 Stipp, M., Stünitz, H., Heilbronner, R., and Schmid, S.M., 2002. The eastern Tonale fault  
1168 zone: a 'natural laboratory' for crystal plastic deformation of quartz over a  
1169 temperature range from 250 to 700 °C. *Journal of Structural Geology* 24, 1861-  
1170 1884.
- 1171 Tapponnier, P., Peltzer, G., and Armijo, R., 1986. On the mechanics of the collision  
1172 between India and Asia. In: Coward, M.P., and Ries, A.C., (eds), *Collision*  
1173 *Tectonics*, Geological Society Special Publication 19, 115-157.
- 1174 Tapponnier, P., Peltzer, G., Le Dain, A.Y., Armijo, R., and Cobbold, P., 1982.  
1175 Propagating extrusion tectonics in Asia: New insights from simple experiments  
1176 with plasticine. *Geology* 10, 611-616.

- 1177 Upton, D.R., 1999. A regional fission track study of Thailand: implications for thermal  
1178 history and denudation. Unpublished PhD Thesis, Royal Holloway University of  
1179 London, UK, 392 pp.
- 1180 van der Voo, R., Spakman, W., and Bijwaard, H., 1999. Tethyan subducted slabs under  
1181 India. *Earth and Planetary Science Letters* 171, 7-20.
- 1182 Wang, E., Burchfiel, B.C., Royden, L.H., Liangzhong, C., Jishen, C., Wenxin, L., and  
1183 Zhiliang, C., 1998. Late Cenozoic Xianshuihe-Xiaojiang, Red River, and Dali  
1184 fault systems of Southwestern Sichuan and Central Yunnan, China. Boulder,  
1185 Colorado, Geological Society of America Special Paper 327, 108pp.
- 1186 Zaw, K., 1990. Geological, petrological and geochemical characteristics of granitoid  
1187 rocks in Burma: with special reference to the associated W–Sn mineralisation and  
1188 their tectonic setting. *Journal of Southeast Asian Earth Sciences* 4, 293–335.  
1189  
1190

1191 **Figure captions**

1192 **Fig. 1.** Regional tectonic elements of mainland Southeast Asia. Horizontal line ornament:  
1193 Western Province granites; dotted ornament: Main Range granites; vertical line  
1194 ornament: Eastern Province granites; pale grey: Tertiary basins; black lines: brittle faults;  
1195 grey half arrows: ductile shear sense; black half arrows: brittle shear sense. After  
1196 Cobbing et al. (1986); Morley (2002); Polachan (1988).

1197

1198 **Fig. 2.** Detail of the Thai Peninsula showing the Ranong and Khlong Marui fault zones.  
1199 (a.) Fault map. Ornament as before, except dark grey: metamorphic cores. Granite  
1200 outlines modified from Department of Mineral Resources (1982), and basin outlines from  
1201 Intawong (2006). (b.) SRTM (Shuttle Radar Topography Mission) digital elevation  
1202 model of the same area.

1203

1204 **Fig. 3.** Field photographs from the KMF and RF, all except (b.) looking onto sub-  
1205 horizontal surfaces. (a.) Weakly stretched pebble in metasediments sheared during  $D_1$ .  
1206 Faint pressure shadows indicate dextral shear sense. (b.) Road cut section near La-Un on  
1207 the RF showing large scale kink band in  $S_1$ , formed at the end of  $D_1$ . (c.) Outcrop of  
1208 characteristic stromatic migmatite from the high melt volume migmatites of the RF, at the  
1209 Myanmar border NW of Tha Sae. Pen is 159 mm long. (d.) S-C' fabric developed in a  
1210 greenschist facies granite mylonite near Ban Set Takuat, Ranong. (e.) Typical ellipsoidal  
1211 boudins of leucosome in a river polished section of low melt migmatites from the isolated  
1212 ductile core north of Kapoe, in the RF. (f.) River polished section showing disharmonic,



1213 rootless folding of a thin leucosome band in the low melt migmatites from the eastern  
1214 side of the KMF ductile core.

1215

1216 **Fig. 4.** Map of the RF ductile core which truncates the pre-D<sub>2</sub> Ranong Granite at Ranong.  
1217 Granite and sedimentary geology modified after Department of Mineral Resources (1982,  
1218 1992). Bold asterisks indicate tie points used to calculate sinistral displacement. See  
1219 sections 3.3 and 4.1 for details. D<sub>1</sub> and D<sub>2</sub> equal area southern hemisphere stereonet  
1220 show poles to ductile foliation (open circles) and ductile lineations (filled circles). D<sub>3</sub> and  
1221 D<sub>4</sub> stereonets show poles to fault planes (open circles) and slickenside lineations (filled  
1222 circles). Section A-A' shows a representative section through the core. Folding is  
1223 schematic and illustrates style and intensity. Dashed lines: foliation in metamorphic  
1224 rocks, bedding in sedimentary rocks; bold lines: main strike-slip faults. All kinematic  
1225 indicators refer to D<sub>3</sub> faults. For location see Fig. 2.

1226

1227 **Fig. 5.** Map of the RF ductile core north of Ban Pak Chan. Details as for Fig. 4, except  
1228 sedimentary geology modified after Department of Mineral Resources (2006).

1229

1230 **Fig. 6.** Map of the RF ductile cores west of Bang Saphan Noi. Details as for Fig. 4.

1231

1232 **Fig. 7.** Map of the KMF ductile core: Khao Phanom, north-east of Phang Nga. Details as  
1233 for Fig. 4.

1234

1235 **Fig. 8.** Field photographs of brittle structures in the KMF and RF. All except (a.) and (c.)  
 1236 looking onto sub-horizontal surfaces. (a.) Limestone mountains north of Thap Put,  
 1237 marking the trace of a steeply dipping  $D_3$  minor strand of the KMF. (b.) Polished section  
 1238 of weakly foliated fault breccia from a  $D_3$  brittle strand within the KMF ductile core at  
 1239 Khao Phanom. Clasts are mostly fragments of  $D_2$  mylonite, found in nearby intact units.  
 1240 (c.) Fault plane showing an older sinistral strike-slip fault with a small reverse oblique  
 1241 component, reactivated in a normal sense. Exposed within a 2 m wide zone of cataclasis  
 1242 near the northwestern edge of the KMF. (d.) Minor sinistral fault (marked by dashed line)  
 1243 associated with  $D_3$  on the RF west of Bang Saphan Noi. Pale offset surface is a migmatite  
 1244 leucosome. Pen for scale below fault plane. (e.) En-echelon Riedel fault array formed  
 1245 during  $D_4$  showing a slight dextral offset of the banded mylonites through which it cuts.  
 1246 RF, north of Ban Pak Chan. (f.) Quartz segregation in KMF quartz-biotite mylonites,  
 1247 showing a dextral offset along a typically oblique  $D_4$  fault.

1248

1249 **Fig. 9.** Transect through the ductile core at Khao Plai Khlong Hin Phao north of Ban Pak  
 1250 Chan.  $D_1 - D_2$  foliation shown by dip and strike symbols. Bold lines indicate major  $D_3$   
 1251 faults. Small fault maps illustrate typical  $D_4$  structures developed in all lithologies. Pale  
 1252 grey bands represent deformed foliation parallel ductile markers such as stromatic  
 1253 leucosomes and stretched objects.  $D_4$  fault scale bars are 10 cm long. Whole map and  $D_4$   
 1254 figures rotated  $20^\circ$  anticlockwise.

1255

1256 **Fig. 10.** Regional reconstruction in Late Cretaceous times. Based on Charusiri et al.  
 1257 (1993); Hall (2002); Mitchell (1993); Mitchell et al. (2007); Morley (2002); Searle et al.

1258 (2007). After restoration of Neogene movements on the Sagaing Fault and Andaman Sea,  
1259 Western Burma lies outboard of Northern Thailand, close to the KMF and RF. The  
1260 change from an inactive trench offshore Sumatra to active subduction offshore Western  
1261 Burma is adjacent to the position of the KMF.

1262

1263 **Fig. 11.** Schematic block diagram illustrating major processes during deformation of the  
1264 KMF and RF. Metamorphic fault rocks of one or more ductile shear zones, indicated by  
1265 grey shading, cut and are cut by granitoid intrusions, and contain foliation parallel syn-  
1266 kinematic intrusions at deeper levels. Post kinematic granites are widespread, and are  
1267 emplaced outside the main fault zone. Transpressive sinistral faulting during  $D_3$  forces  
1268 slivers of the older shear zone to the surface in positive flower structures, which cross cut  
1269 all older features. These brittle faults may be rooted in ductile shear zones at depth. Grey  
1270 kinematic indicators represent  $D_1 - D_2$ , black represents  $D_3$ .

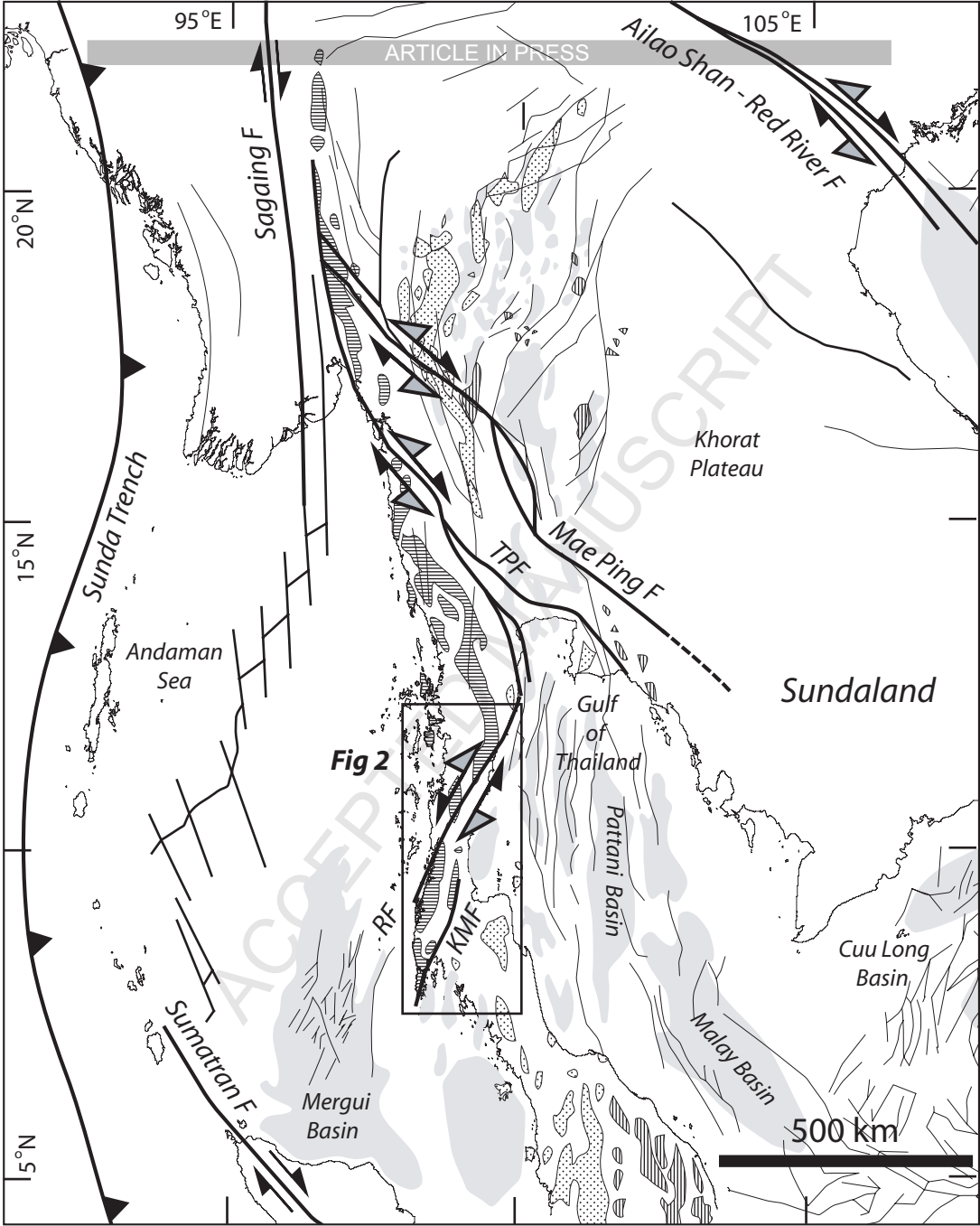
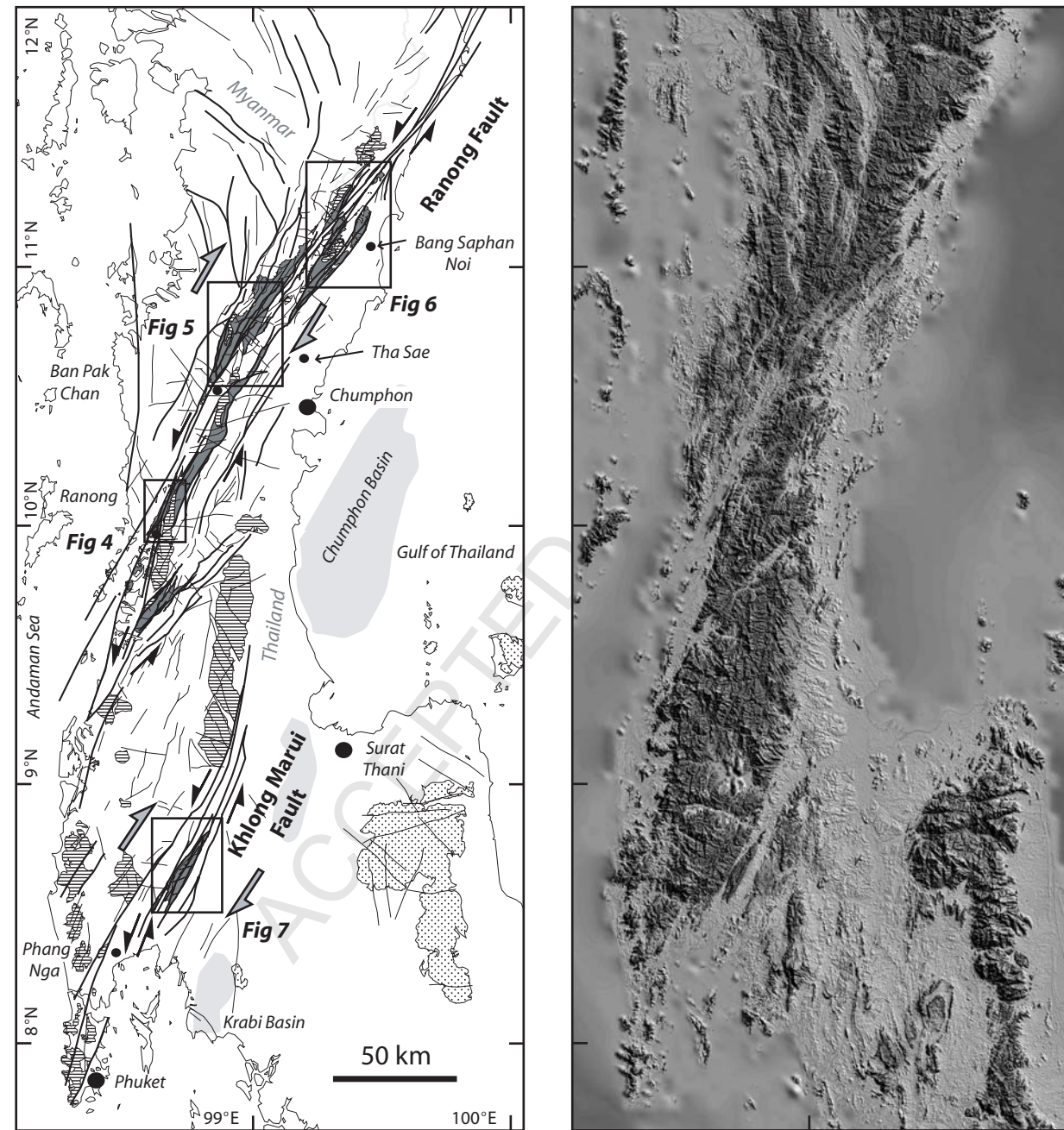


Figure 1



a.)

b.)

Figure 2

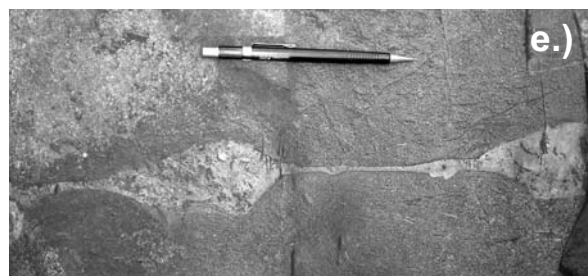
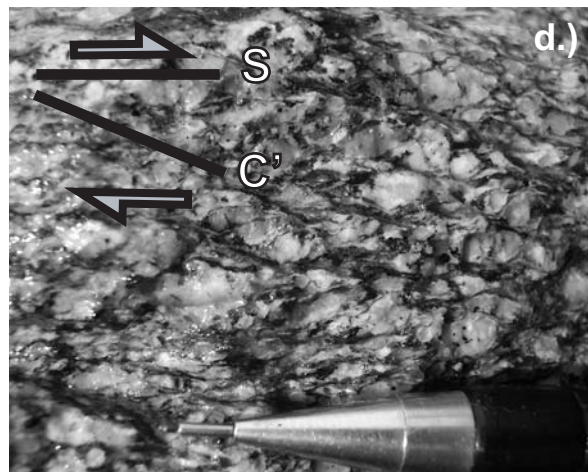
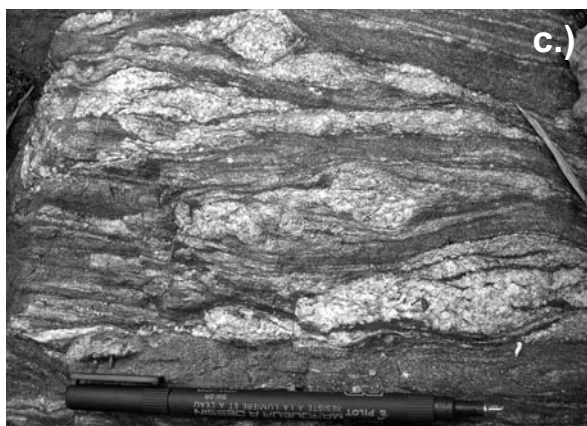
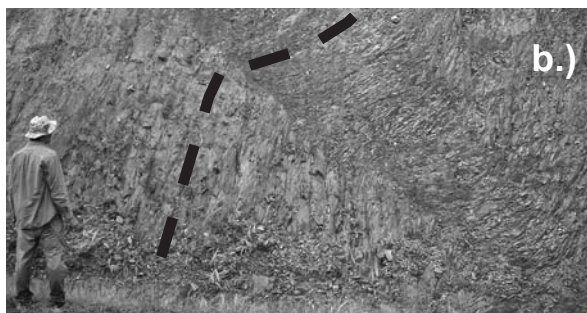
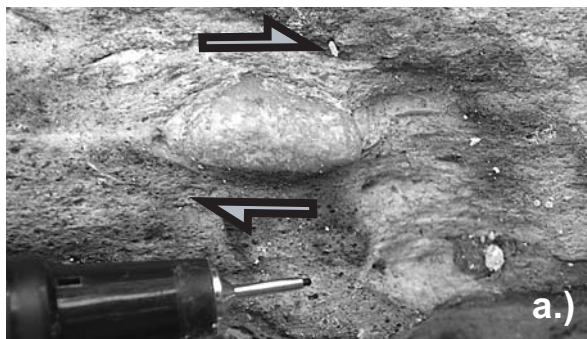


Figure 3

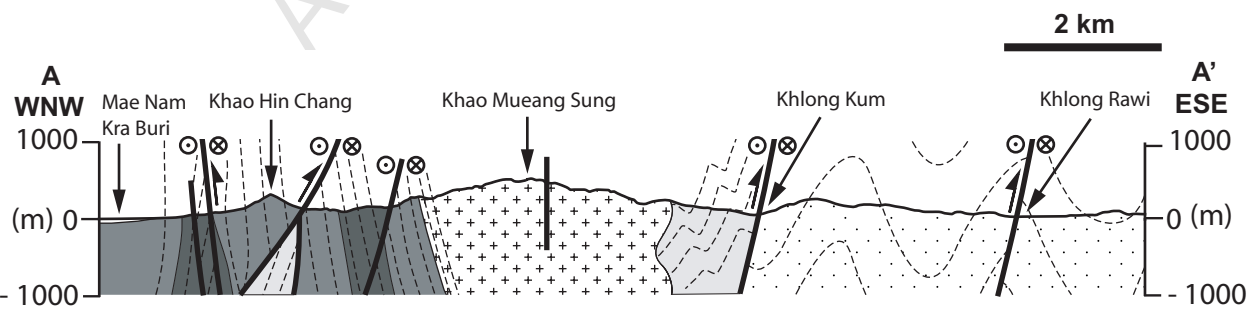
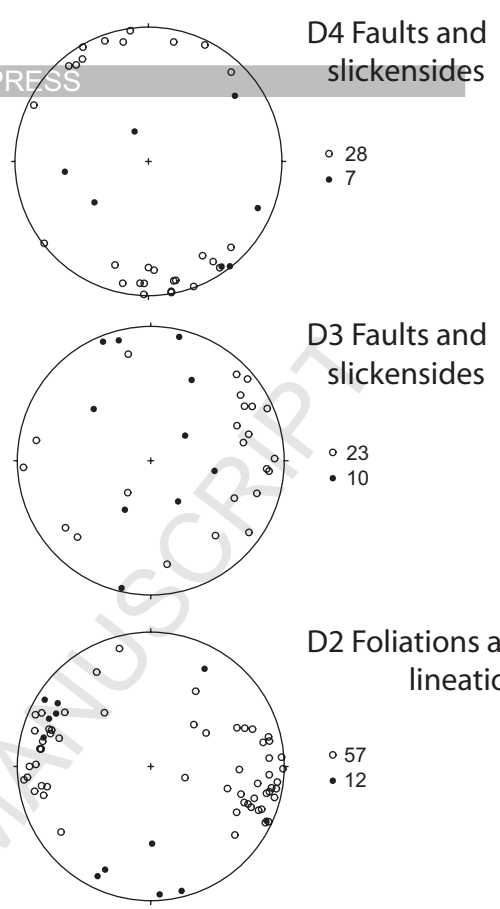
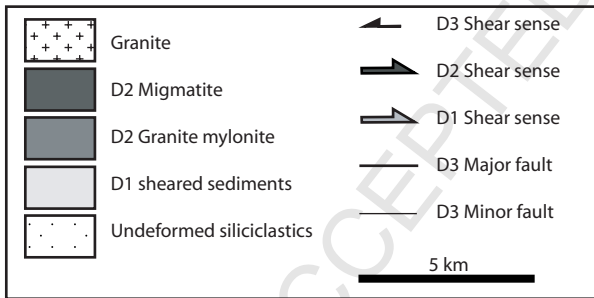
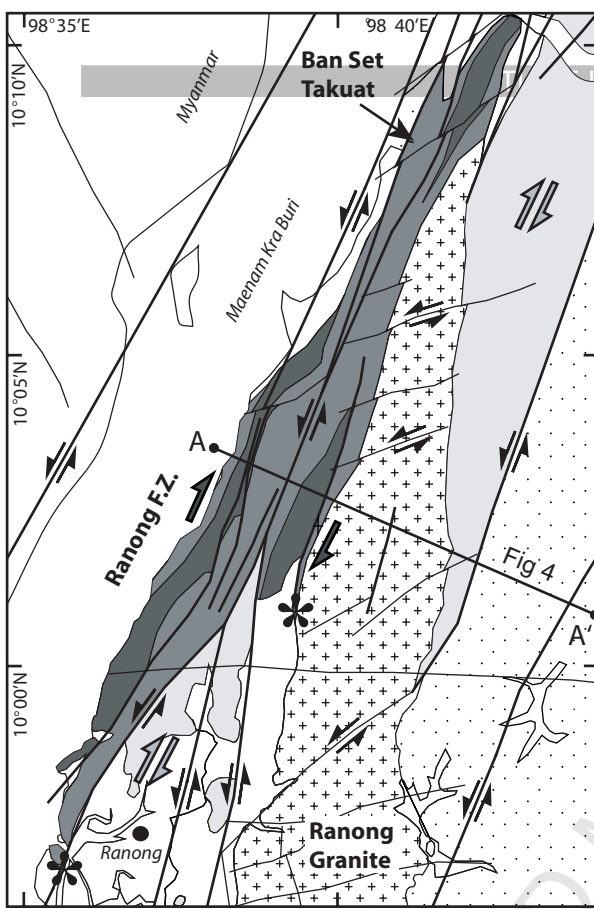
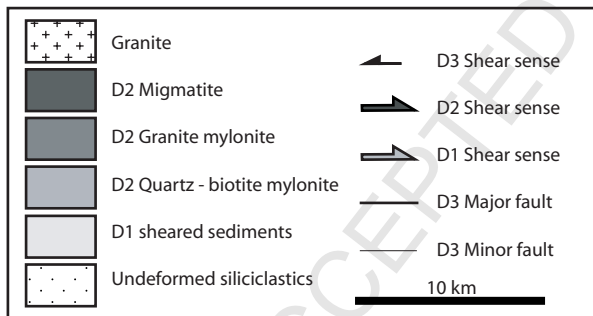
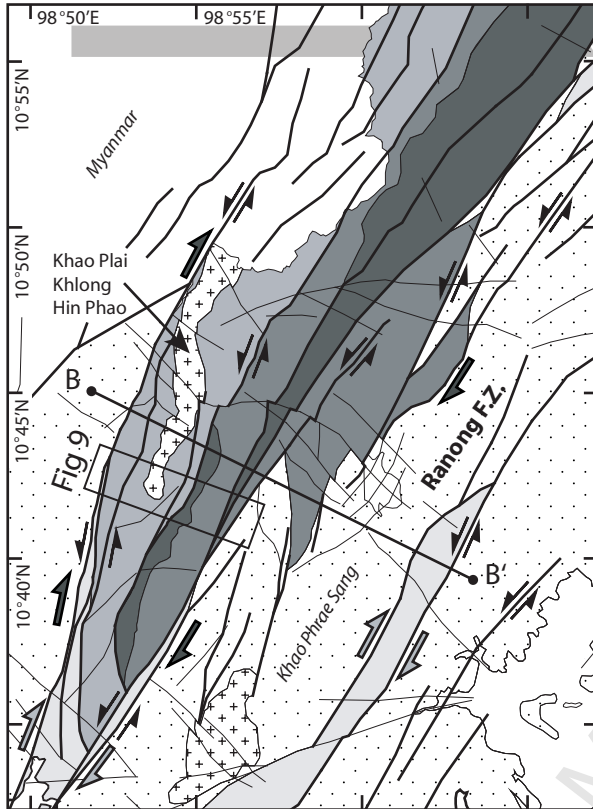
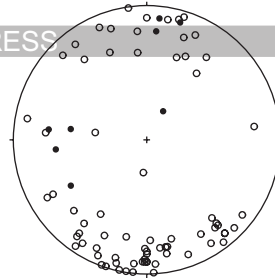


Figure 4



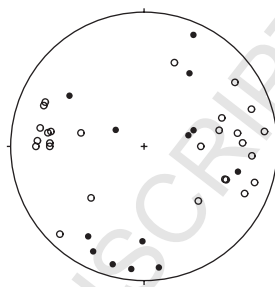
ACCEPTED MANUSCRIPT  
PRESS

D4 Faults and slickensides



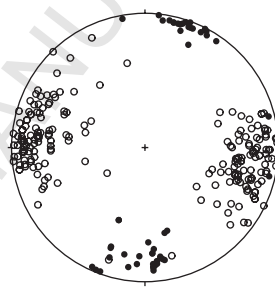
○ 73  
● 8

D3 Faults and slickensides



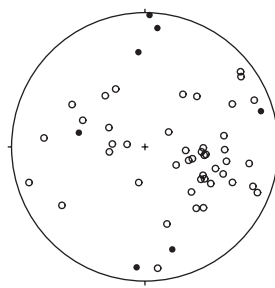
○ 27  
● 13

D2 Foliations and lineations



○ 207  
● 53

D1 Foliations and lineations



○ 45  
● 7

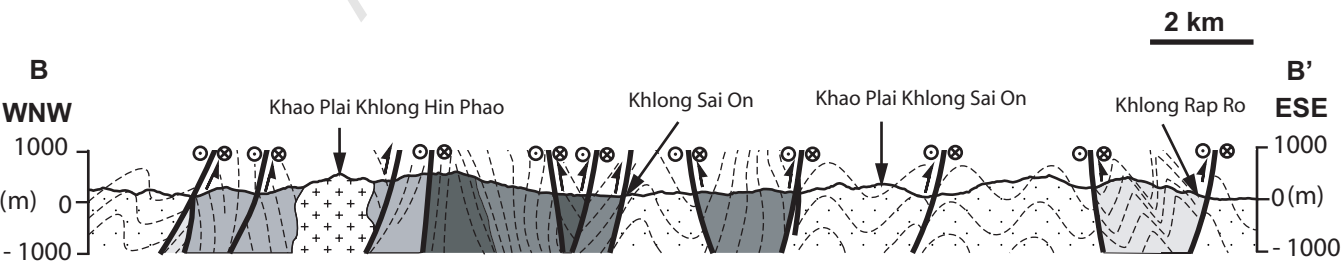


Figure 5



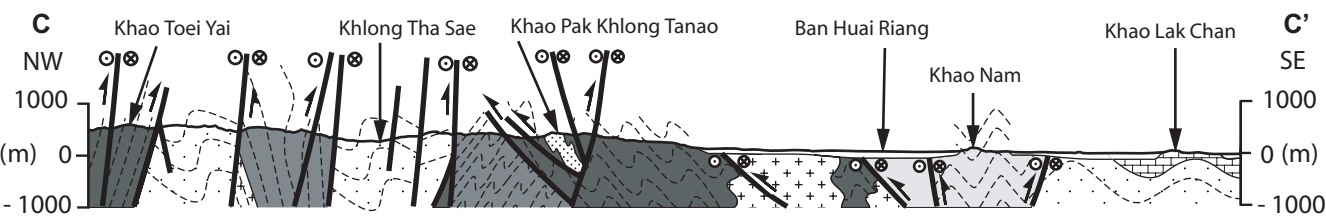
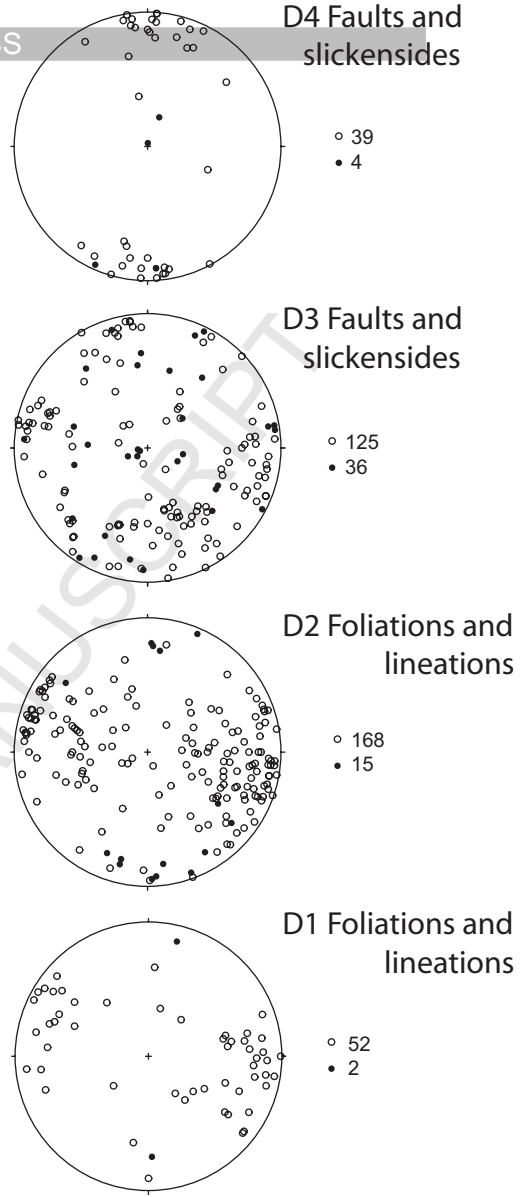
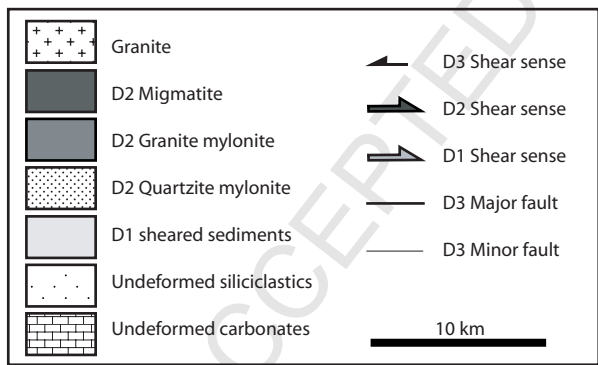
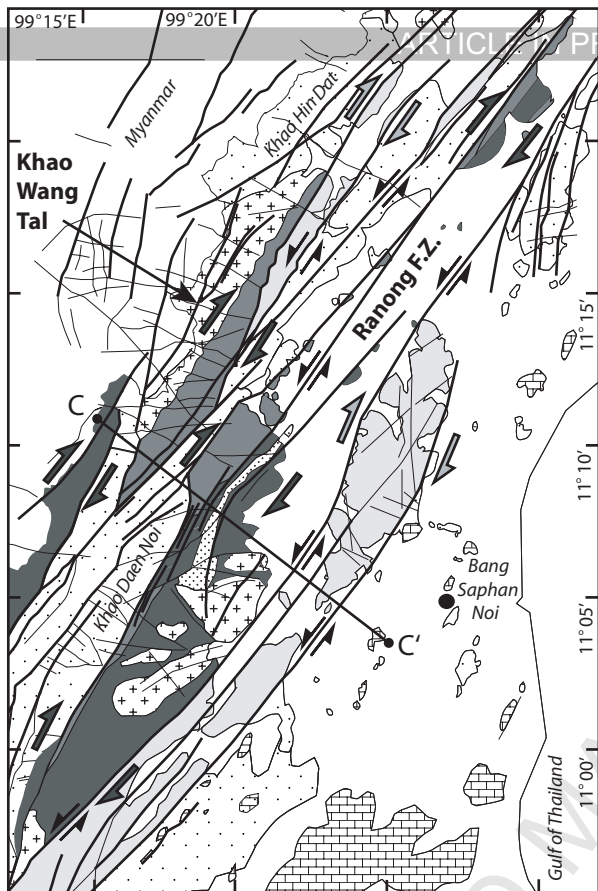
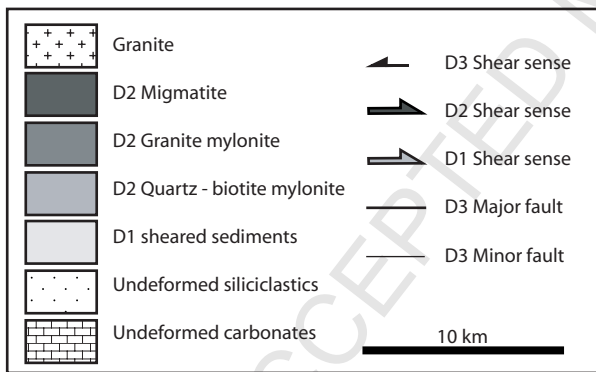
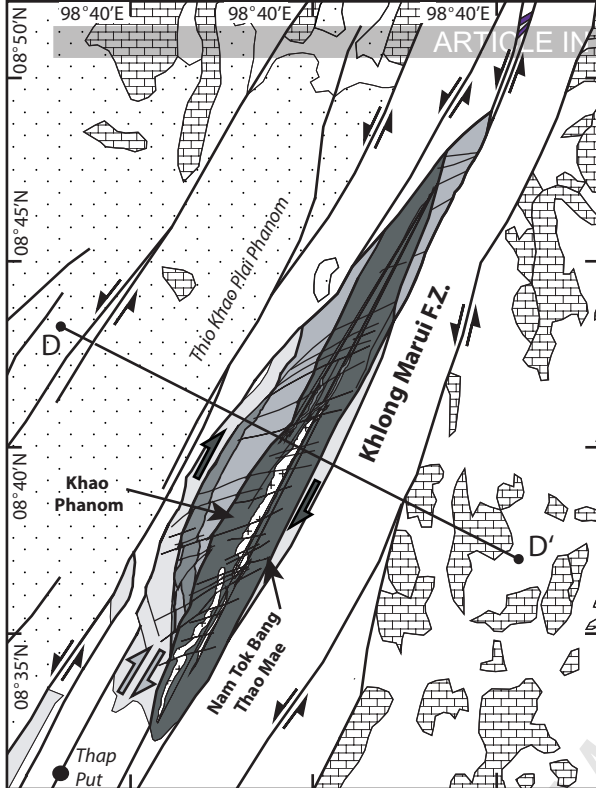
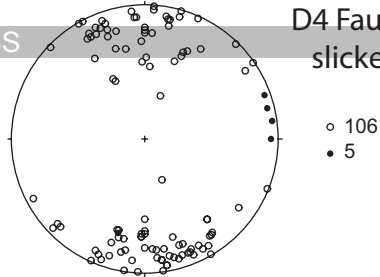


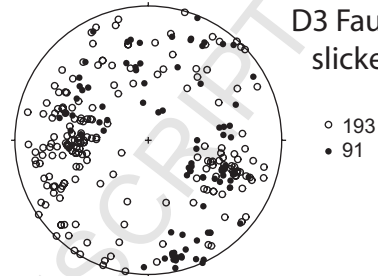
Figure 6



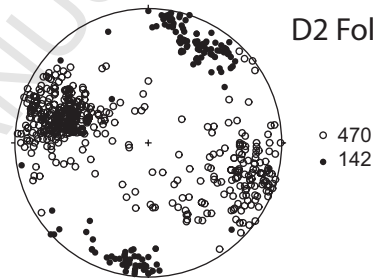
### D4 Faults and slickensides



### D3 Faults and slickensides



### D2 Foliations and lineations



### D1 Foliations and lineations

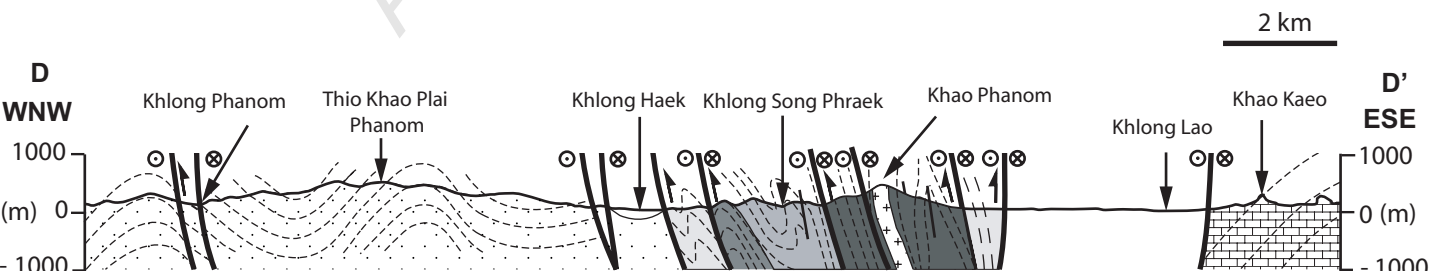
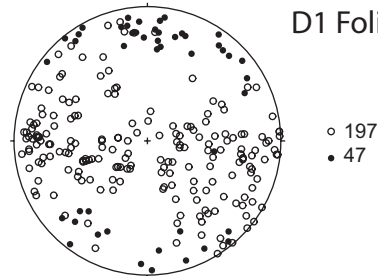


Figure 7

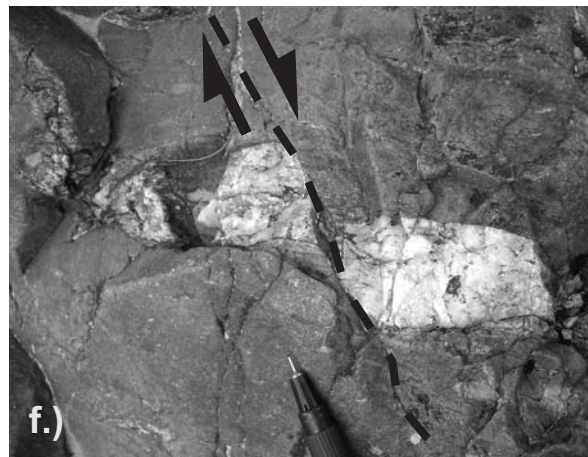
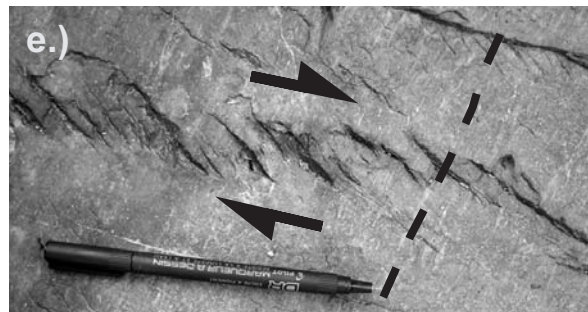
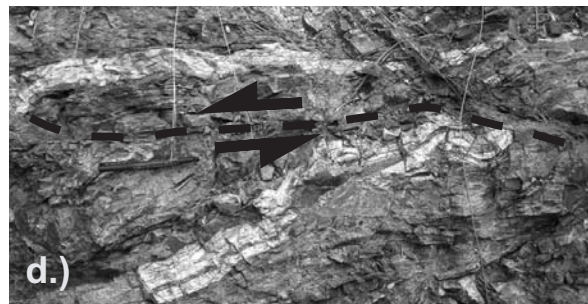
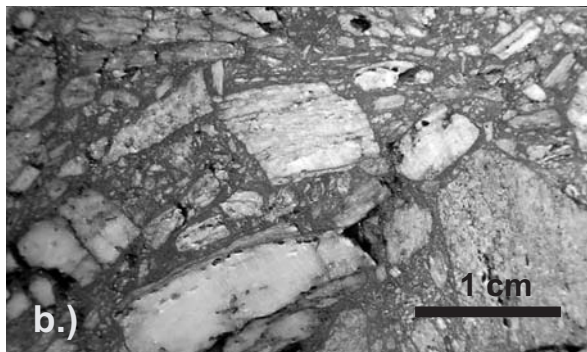


Figure 8

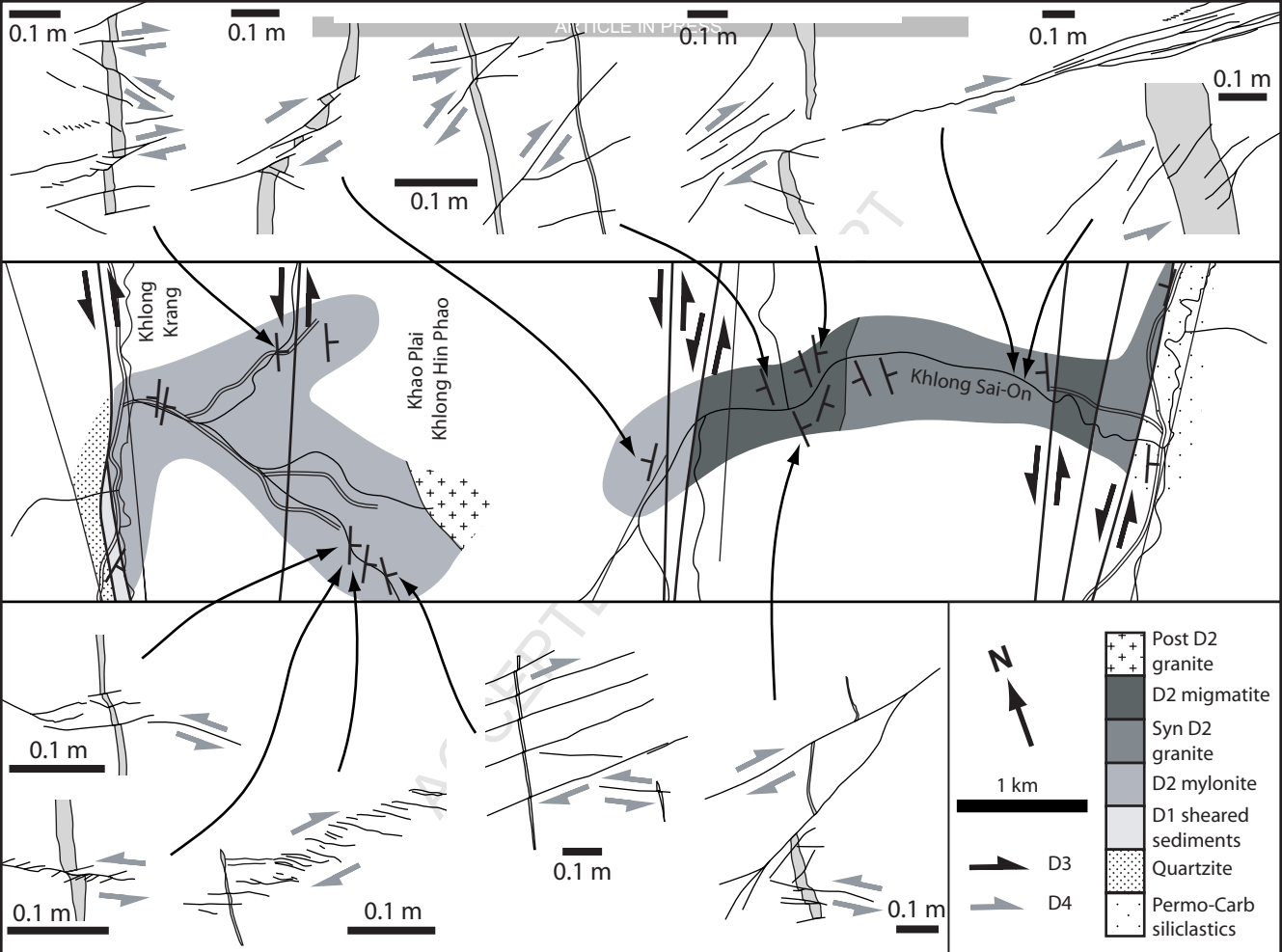


Figure 9

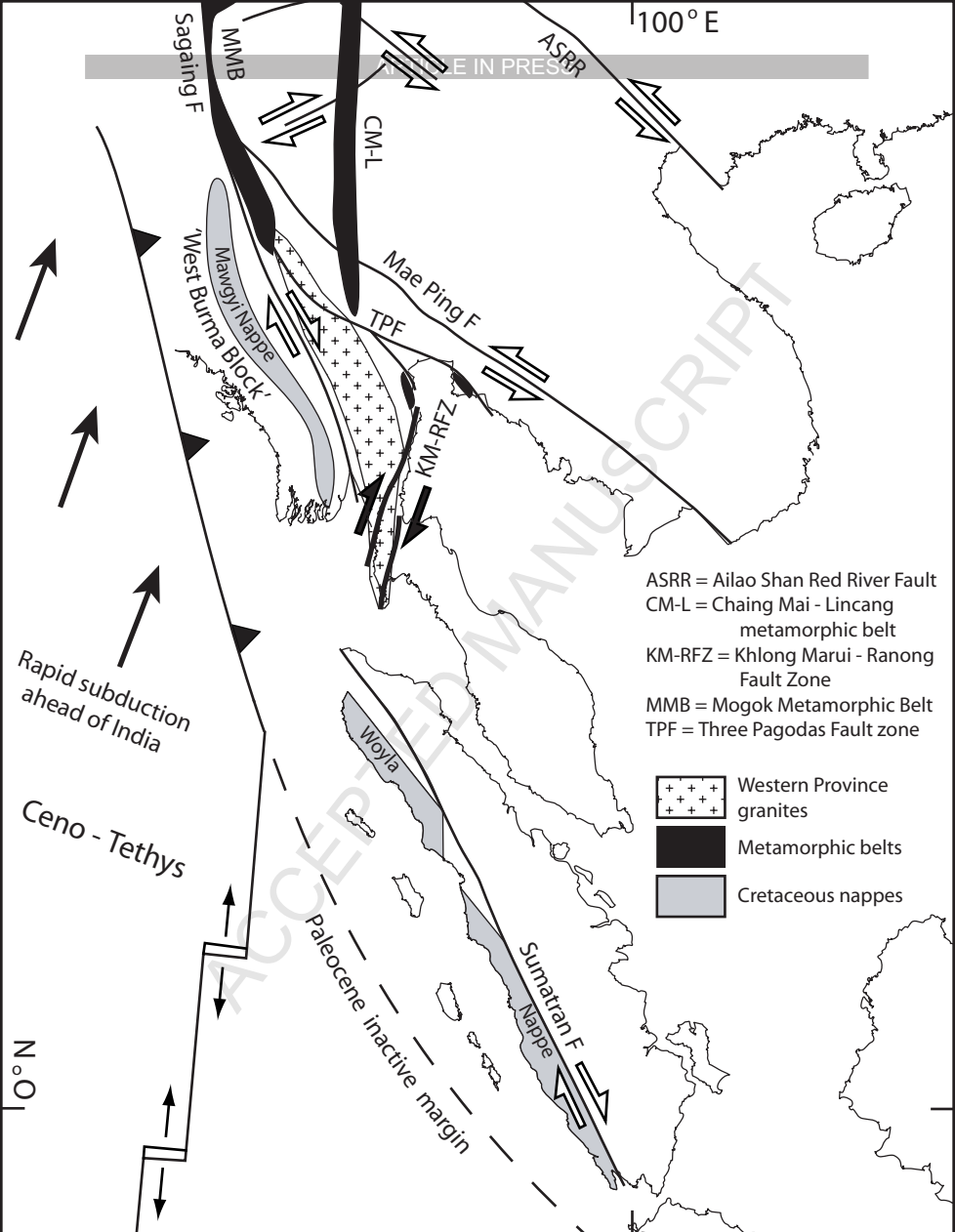


Figure 10

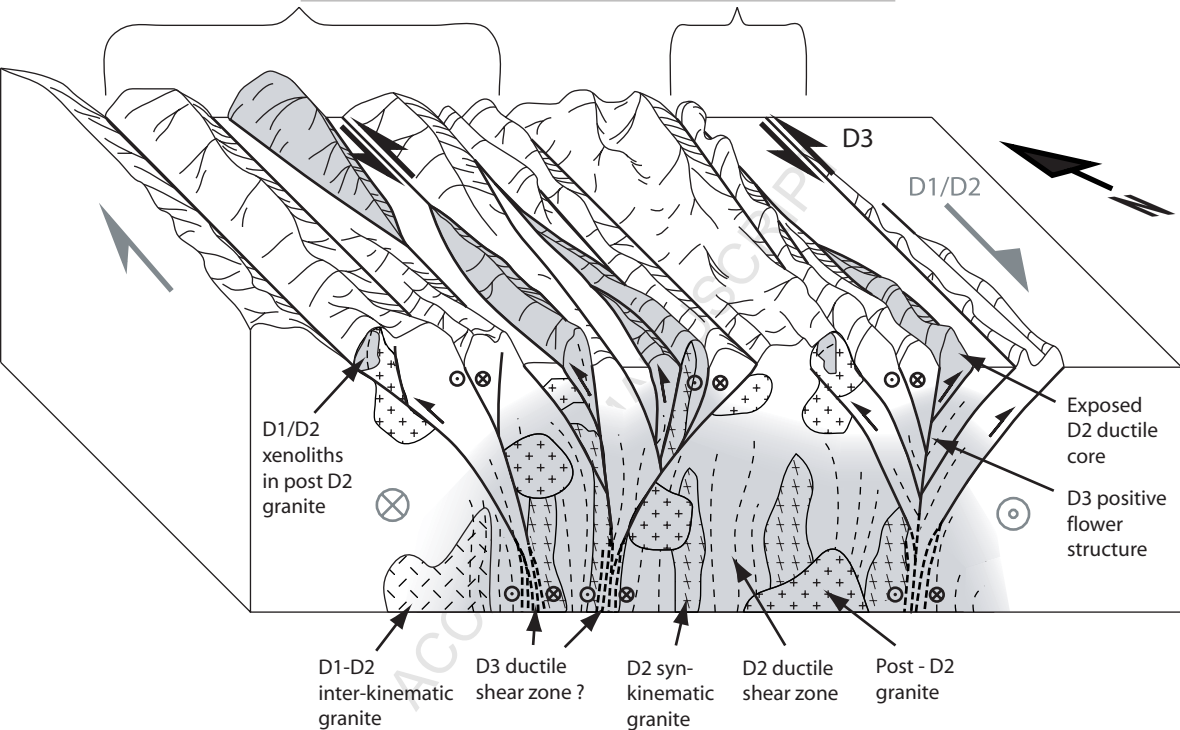


Figure 11